

8 Appendices

Table of Contents (Appendices)

8	Appendices	1
8.1	Chapter 2 appendices	5
8.1.1	Gateway Cloning Protocol	7
8.1.1.1	Primer Design	7
8.1.1.2	PCR conditions	7
8.1.1.3	BP cloning and subsequent cloning stages	7
8.2	Chapter 3 appendices	8
8.3	Chapter 4 appendices	19
8.4	Chapter 5 appendices	34
8.5	Chapter 6 appendices	53

List of Figures

Figure 8-1: Summary of the genome wide bioinformatics analysis	10
Figure 8-2: Induction with tetracycline does not affect cell growth or γ H2A expression (under genotoxic stress conditions) of the 2T1 RNAi parental cell line	12
Figure 8-3: <i>In vitro</i> growth analysis of the false positive candidates	13
Figure 8-4: <i>In vitro</i> cell cycle analysis of genome wide candidates at 12 hours post induction	14
Figure 8-5: Confirmation of TbKFR1 ^{+/-12myc} clones	15
Figure 8-6: TbKFR1 localisation following MMS exposure	16
Figure 8-7: Kinome wide candidate localisation in the presence or absence of MMS	18
Figure 8-8: Protein sequence alignments between TbAUK2, AUKA and c-Src ----	21
Figure 8-9: Protein sequence alignments between the <i>T. brucei</i> aurora kinases	23
Figure 8-10: Additional examples of nuclei imaged by TEM from TbAUK2 -/- cells	24
Figure 8-11: <i>In vitro</i> growth of TbAUK2 +/- cell lines following treatment with DNA damaging agents	26
Figure 8-12: Anti myc antiserum does not bind non-specifically to WT427 cells	27
Figure 8-13: TbAUK2 fails to localise in a population of cells	28
Figure 8-14: Super resolution imaging of WT427 cells stained with anti myc antiserum	29
Figure 8-15: Localisation of TbAUK2 after HU, UV and PHL exposure	30
Figure 8-16: Loss of TbAUK2 is not associated with expression of silent VSG RNA transcripts	32
Figure 8-17: Overexpression of TbAUK2 does not affect cellular proliferation or increase sensitivity to MMS	33
Figure 8-18: Amino acid sequence alignments between the Tb6560 TREU 927 and Lister 427 sequences	35
Figure 8-19: Full amino acid sequence alignments between the Tb6560 TREU 927 sequence and the putative homologues in other organisms	39
Figure 8-20: Amino acid sequence alignments between the Tb6560 TREU 927 sequence and the putative orthologues in other kinetoplastid parasites	42
Figure 8-21: PCR analysis of putative Tb6560 heterozygote (+/-) clones	43
Figure 8-22: Tb6560 localisation following cytoskeleton extraction	44
Figure 8-23: <i>In vitro</i> growth analysis of Tb6560 +/- cells under genotoxic stress	45
Figure 8-24: Expression of γ H2A in WT and Tb6560 null mutant cells	46
Figure 8-25: Tb6560 localisation following DNA damage exposure	47
Figure 8-26: Tb6560 +/- cells images by TEM	48
Figure 8-27: TbBILBO-1 localisation in Tb6560 null mutant cell lines	49
Figure 8-28: Cells lacking Tb6560 are defective in endocytosis	51
Figure 8-29: Protein sequence alignments between TbATR, Mec1 and human ATR	58
Figure 8-30: Protein sequence alignments between TbATM, the budding yeast ATM and human ATM	65
Figure 8-31: TbATR and TbATM shows structural similarity to	67
Figure 8-32: <i>In vitro</i> cell cycle analysis of TbATR	68
Figure 8-33: Loss of TbATR is associated with increased γ H2A expression in BSF cells	69

List of Tables

Table 8-1: Primers used for Gateway cloning	6
Table 8-2: RNAi cell lines used from false positive candidates.....	11
Table 8-3: Primers used to generate TbKFR1 heterozygote (+/-) cell lines	15
Table 8-4: Additional 'hits' retrieved from the SmartBLAST analysis	20
Table 8-5: Concentrations of RNA from each sample used for the RNAseq experiment.	70
Table 8-6: FlagStat analysis of the individual RNAseq replicates	71

8.1 Chapter 2 appendices

The following section contains the additional material referenced in Chapter 2 (Materials and Methods).

Primer Number	Plasmid (pTL)	Gene ID	Gene Name	Primer Sequence 5' -- 3'
TL099	pTL50	Tb927.11.14680	TbATR	GGGGACAAGTTTGTACAAAAAAGCAGGCTTAACGCTCCCTTAAGTGCAAAA
TL0100				GGGGACCACCTTGTACAAGAAAGCTGGGTGAATTCCTCCAATGAAGAA
TL0321	pTL161	Tb927.9.6560	Tb6560	GGGGACAAGTTTGTACAAAAAAGCAGGCTCTCTGCTCTCGAGACTG
TL0322				GGGGACCACCTTGTACAAGAAAGCTGGGTAGAGGTCATCCGTTGTTGGT
TL0371	pTL186	Tb927.2.1820	TbCAMK	GGGGACAAGTTTGTACAAAAAAGCAGGCTACGGCTCGGCTATACTTTCA
TL0372				GGGGACCACCTTGTACAAGAAAGCTGGGTAGATCCGTTTGAAACCACGG
TL0211	pTL106	Tb927.10.7780	TbKFR1	GGGGACAAGTTTGTACAAAAAAGCAGGCTCAAATTGCTATGCCGTTGC
TL0212				GGGGACCACCTTGTACAAGAAAGCTGGGTAGCAAAGTAAGGGTGCTGCA
TL0307	pTL154	Tb927.3.3920	TbAUK2	GGGGACAAGTTTGTACAAAAAAGCAGGCTAAACCGAAGGTTGTGATCCA
TL0308				GGGGACCACCTTGTACAAGAAAGCTGGGTGAGAAATATTTCCGGCTTT
TL0333	pTL167	Tb927.8.7220/Tb927.4.5180	TbTLK1/2	GGGGACAAGTTTGTACAAAAAAGCAGGCTGAAAGCCTTGACTTGCAAGG
TL0334				GGGGACCACCTTGTACAAGAAAGCTGGGTATGGTTGGGTTGTCGCTTG
TL0149	pTL75	Tb927.11.1180	TbCRK6	GGGGACAAGTTTGTACAAAAAAGCAGGCTAGTGACAAGCTGAAGGAAGG
TL0150				GGGGACCACCTTGTACAAGAAAGCTGGGTGGTGACGATACCACAACG
TL0209	pTL105	Tb927.7.960		GGGGACAAGTTTGTACAAAAAAGCAGGCTCTCCTCAGAAGGCCAGTACG
TL0210				GGGGACCACCTTGTACAAGAAAGCTGGGTGCCGACTGGAGCAAAAAGAA
TL0141	pTL71	Tb927.6.3110	TbCRK11	GGGGACAAGTTTGTACAAAAAAGCAGGCTCCGTTTGTGTCATGAGACTG
TL0142				GGGGACCACCTTGTACAAGAAAGCTGGGTACGTTTCTTGGGATCCACTT
TL0201	pTL101	Tb927.10.5140	TbMAPK2	GGGGACAAGTTTGTACAAAAAAGCAGGCTCGCTTGAAAAGGAGCAAGTG
TL0202				GGGGACCACCTTGTACAAGAAAGCTGGGTACTCTTGTCATGGTGAAGCGG
TL0147	pTL74	Tb927.8.5390	TbCRK4	GGGGACAAGTTTGTACAAAAAAGCAGGCTATATAACGCATTATCGTCGG
TL0148				GGGGACCACCTTGTACAAGAAAGCTGGGTACAGTACCATCGGCTCCATG
TL015	pTL8	Tb927.10.1380	TbNEK19	GGGGACAAGTTTGTACAAAAAAGCAGGCTGTTGTGGGTCGAGATCCAGT
TL016				GGGGACCACCTTGTACAAGAAAGCTGGGTGACATGAATTTGAGCGAGCA
TL0265	pTL133	Tb927.10.5270	TbMMK5	GGGGACAAGTTTGTACAAAAAAGCAGGCTAAAGTTTACAGGTCAAACCC
TL0266				GGGGACCACCTTGTACAAGAAAGCTGGGTTTCAGCAACAGCAAGACCAA
TL0217	pTL109	Tb927.8.5950	TbSTE	GGGGACAAGTTTGTACAAAAAAGCAGGCTGTCGACGGGTAAAGGTGAAAC
TL0218				GGGGACCACCTTGTACAAGAAAGCTGGGTCCCCATCGGAGAGCTTCTT
TL0199	pTL100	Tb927.10.12040	TbMAPK11	GGGGACAAGTTTGTACAAAAAAGCAGGCTATTCTTGTTGAGTTGCTGG
TL0200				GGGGACCACCTTGTACAAGAAAGCTGGGTCTCTCATCATACCCGCCA
TL0277	pTL139	Tb927.10.8730	TbABC1	GGGGACAAGTTTGTACAAAAAAGCAGGCTTTGTAAAGGTGATGCACCCA
TL0278				GGGGACCACCTTGTACAAGAAAGCTGGGTGTCGAGGCGTCAATAATAA
66	N/A	Tb927.2.2260	TbATM	GGGGACAAGTTTGTACAAAAAAGCAGGCTGGACGCAACTGAGGAAGAAAG
67				GGGGACCACCTTGTACAAGAAAGCTGGGTACGCTGTCCAGAAGTTGAA

Table 8-1: Primers used for Gateway cloning
pTL refers to Mottram lab plasmid numbering system. Red= FW *attB* site sequence. Blue = RV *attB* site sequence.

8.1.1 Gateway Cloning Protocol

The following protocol was designed by N.Jones.

8.1.1.1 Primer Design

Primers for Gateway® cloning were designed using the RNAit software (<http://trypanofan.path.cam.ac.uk/software/RNAit.html>). The following sequences were added to the 5' end of each primer.

FW Primer: 5' GGGGACAAGTTTGTACAAAAAAGCAGGCT - gene specific-3'.

RV Primer: 5' GGGGACCACTTTGTACAAGAAAGCTGGGT - gene specific 3'.

8.1.1.2 PCR conditions

The following master mix was set up for each reactions: 5 x Phusion Buffer 10 µl, 10 mM dNTP mix 1µl, Template DNA 2 µl, ddH₂O 32 µl, Primer one 2.5 µl, Primer two 2.5 µl, Phusion enzyme 0.5 µl. The following ThermoCycler settings were used: 98°C 3 min followed by 30 cycles of (98°C 30 sec, 60°C 30 sec and 72°C 30 sec) and a final extension at 72°C 10 min.

8.1.1.3 BP cloning and subsequent cloning stages

The PCR product was resolved on an agarose gel as per section 2.2.2 and the required fragment gel extracted as per section 2.2.5. A BP reaction was then performed as follows: The entire PCR product was added to a 1.5 ml Eppendorf tube containing the pGL2084 vector (150 ng/µl) 1µl, TE buffer, pH 8.0 3.75 µl and add 0.25 µl of BP Clonase™. The reactions were incubated at room temperature for between 1 hr and overnight. To terminate the BP reaction, 1 µl Proteinase K was added and the samples placed at 37°C for 10 mins. The resulting solution was transformed as detailed in section x using Max efficiency DH5α (Invitrogen) cells. The plasmid was extracted as per section x and diagnostic restriction digest analysis performed on each plasmid using the following enzymes: Ascl, Stul, Clal and BamHI & XbaI. Digested were performed as per section 2.2.6.

8.2 Chapter 3 appendices

The following section contains the additional material referenced in Chapter 3 (Identifying novel DNA repair-associated protein kinases using RITseq screening).

For all raw and processed values referred to in chapter 3, see folder labelled Chapter3RITseqtables and the subsequently enclosed Tables labelled TableS1-S4. The raw RITseq reads are encompassed in the folder within entitled RawRITseqreads.

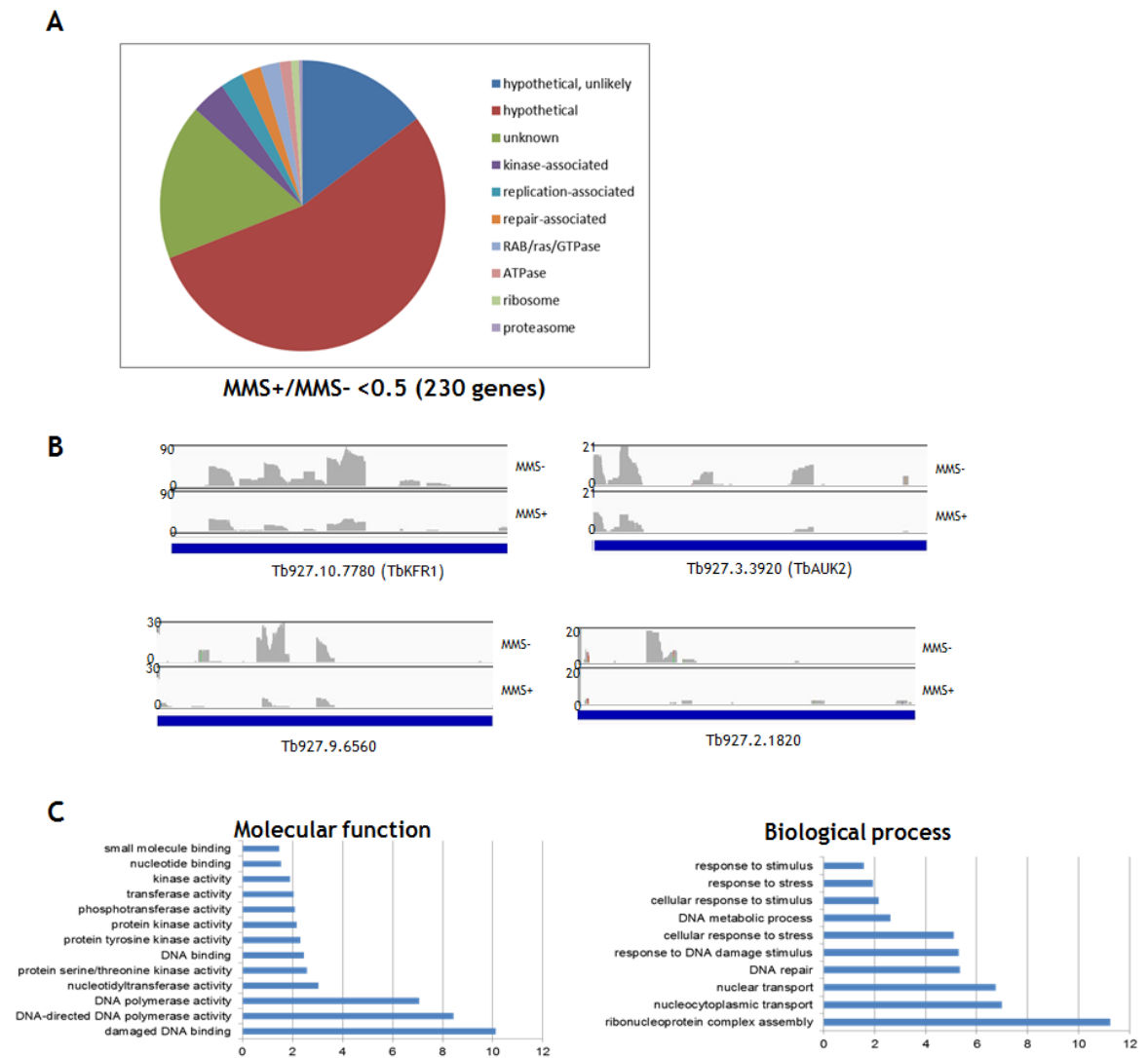


Figure 8-1: Summary of the genome wide bioinformatics analysis

(A) Pie charts summarising the data from the genome wide screen. All 230 genes with MMS+/MMS- ratios of <0.5 were categorised based on their predicted annotation on TriTrypDB.org (v.28). (B) Individual read mapping profiles for four of the genome wide candidates (as labelled in the figure). The read counts from the non-induced or induced samples in the presence of MMS were mapped to the corresponding region in the genome. (C) GO terms enriched from the 230 genes with MMS+/MMS- ratios <0.5. GO terms were retrieved from TriTrypDB based on the gene annotations associated with each gene.

Gene ID	Annotation	Stabilate number	Plasmid number	Puromycin sensitivity
Tb927.8.5390	CRK4	STL610	pTL74	Sensitive
Tb927.10.1380	NEK19	STL0008	pTL8	Sensitive
Tb927.10.5270	MMK5	STL242	pTL133	Sensitive
Tb927.8.5950	STE kinase	STL185	pTL109	Sensitive
Tb927.10.12040	MAPK11	STL684	pTL100	Resistant
Tb927.10.8730	ABC1	STL556	pTL139	Sensitive

Table 8-2: RNAi cell lines used from false positive candidates

Details of the cell lines used for all candidates validated across both screens. STL number = stabilate number according to the Mottram laboratory system for stabilate labelling. pTL = Mottram laboratory plasmid repository numbering system.

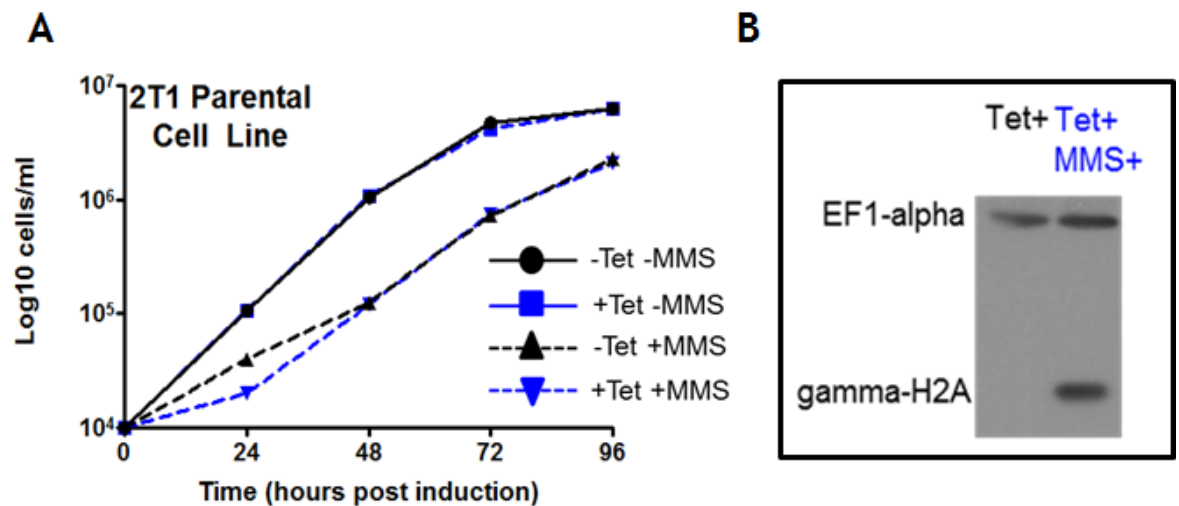


Figure 8-2: Induction with tetracycline does not affect cell growth or γ H2A expression (under genotoxic stress conditions) of the 2T1 RNAi parental cell line

(A) Growth curve over 96 hrs of induced (tet +) and uninduced (tet-) cells in the presence (MMS+) or absence (MMS -) of genotoxic stress (generated by MMS). Every 24 hrs the cell density was assessed as per section 2.8.1. Error bars represent the SEM of two independent experiments. (B) Expression of γ H2A was assessed via western blot analysis as per section 2.12.1. Whole cell lysates were prepared and blotted onto a membrane which was first probed with an anti- γ H2A antibody (T.D.Serafim, unpublished) then the membrane was re-probed with an anti-EF1 alpha antibody as a loading control. Addition of tetracycline to the medium does not result in γ H2A expression (Tet +). In the presence of both tetracycline and MMS (Tet + MMS +) expression of γ H2A can be seen.

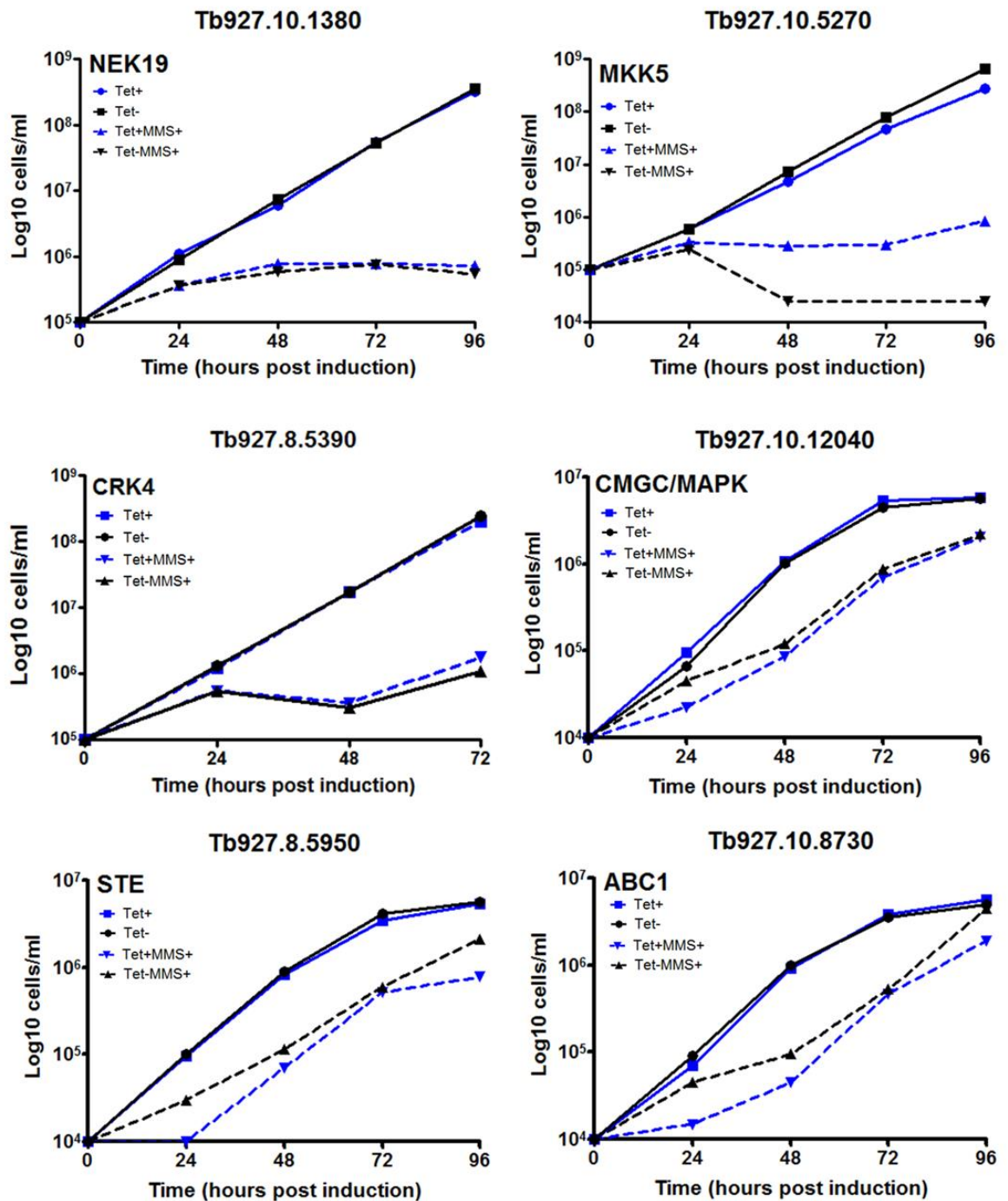


Figure 8-3: *In vitro* growth analysis of the false positive candidates
 Growth analysis of each candidate following RNAi knockdown and following exposure to MMS (0.0003 %). Each growth curve was performed once. Growth curves were performed as detailed in section 2.8.1. Cell lines were induced with $1 \mu\text{g/ml}^{-1}$ tetracycline. Tet+ (solid blue line), Tet- (solid black line), Tet+MMS+ (dashed blue line) and Tet-MMS+ (dashed black line).

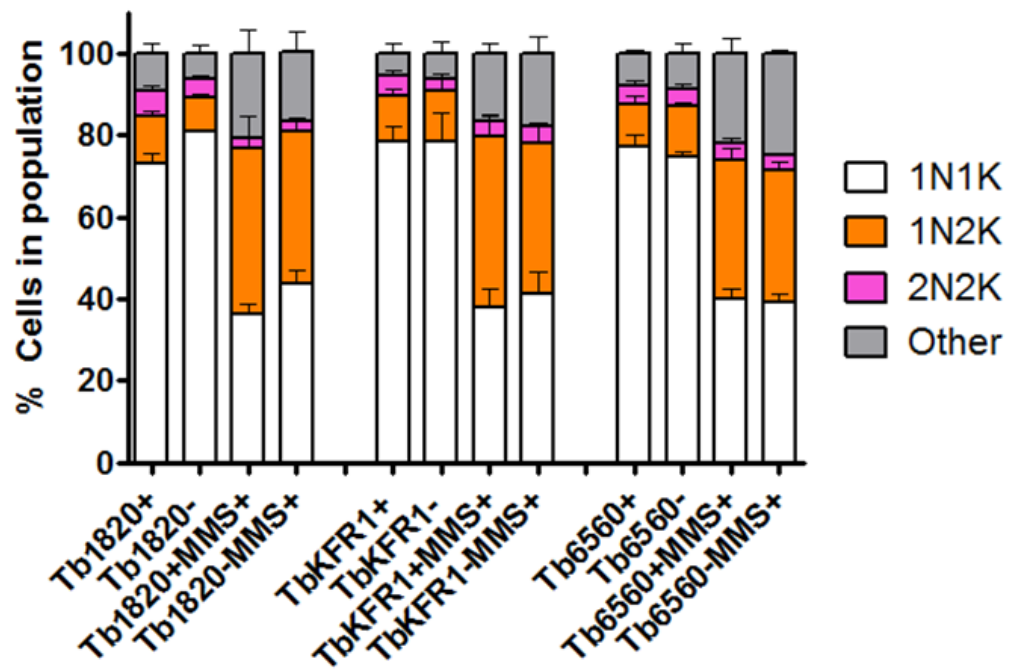


Figure 8-4: *In vitro* cell cycle analysis of genome wide candidates at 12 hours post induction. Cells were induced for 12 hrs with tetracycline, collected as per section 2.8.3 and stained with DAPI as per section 2.11.1 and the number of 1N1K, 1N2K, 2N2K and 'other' cells were counted and expressed as a percentage of the total population. A concentration of 0.0003 % (v/v) MMS was used. The error bars represent \pm SEM (n = 3, > 200 cells counted per experiment). Cells were counted on an Axioskop 2.

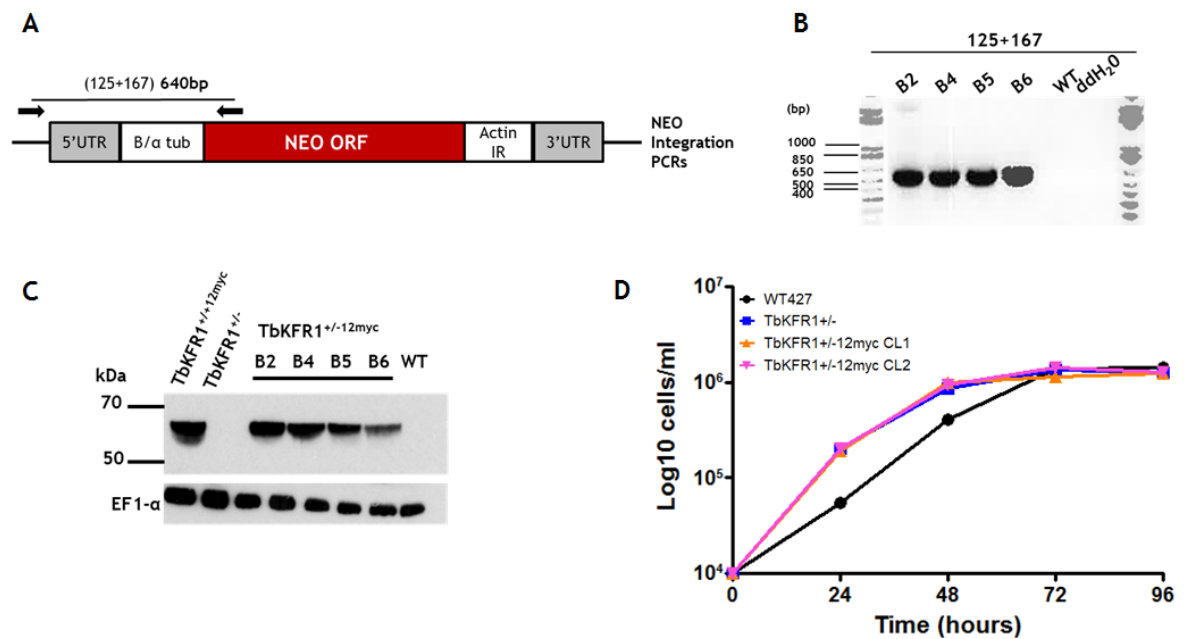


Figure 8-5: Confirmation of $TbKFR1^{+/-12myc}$ clones

(A) Schematic illustration of expected PCR fragment sizes in bold beside which the primers (for sequences refer to Table 2-2; primer 125 sequence: CAAAGACGCAGGAGGAAA) required are detailed in brackets. Black arrows = primer localisation in the genome. Not to scale. (B) Integration PCRs. Images show integration of the $\Delta KFR1::NEO$ construct into endogenously tagged clones. PCRs were all performed on the same gDNA. Fragments of expected sizes were amplified from each clone but not from WT gDNA as expected. ddH₂O was used as a negative control. Amplification of the ORF occurred in all clones and the WT gDNA. Clone B2 (CL1) and B4 (CL2) were chosen. NEO (Neomycin), BSD (Blasticidin), B/α tub (Beta/Alpha Tubulin), Actin IR (Actin intergenic region), WT (Wild type), gDNA (genomic DNA), ddH₂O (double distilled water). Sizes shown (kb plus ladder; bp). (C) Confirmation of endogenously tagged $TbKFR1^{+/-12myc}$ cell lines by western blot analysis. Performed as per section 2.12.2. Membranes were probed with α myc antiserum (to detect the myc epitope) and α EF1α antiserum (as a loading control). (D) *In vitro* growth analysis of $TbKFR1^{+/-12myc}$ cell lines. Growth of $TbKFR1^{+/-12myc}$ cell lines (CL1 and CL2) was assessed as described in section relative to WT and $TbKFR1^{+/-}$. This experiment was performed once.

Disruption of the ORF of one allele of $TbKFR1$ (deleting 1832 bp, from amino acids 50 to 610) was achieved through one round of transformation into $TbKFR1^{+/-12myc}$ cells (WT Lister 427 derived). Cells were transformed with the construct $\Delta KFR1::NEO$ and G418 resistant clones selected (section 2.7.4) to produce putative endogenously tagged heterozygote (+/-) cell lines. The primers used to generate a heterozygote (+/-) cell line are in Table 8-3 below.

Primer Number	Gene	GenelD	Sense	Sequence 5' to 3'	Restriction sites	Use
121	TbKFR1	Tb927.10.7780	FW	GCACG aagctt gcgcccgc TGA AGC AAC GGC AGA ACC	HindIII + NotI	Amplifies 5'UTR region
111	TbKFR1	Tb927.10.7780	RV	GCACG tctaga CAC CAT CTA GTT TTC CTA C	XbaI	
112	TbKFR1	Tb927.10.7780	FW	GCACG gagctc AAC CGT CGA AAG CAA AAG	SacI	Amplifies 3'UTR region
122	TbKFR1	Tb927.10.7780	RV	GCACG atcgat gcgcccgc GGT CAA GAT GAT AGC GGT	Clal + NotI	

Table 8-3: Primers used to generate $TbKFR1$ heterozygote (+/-) cell lines

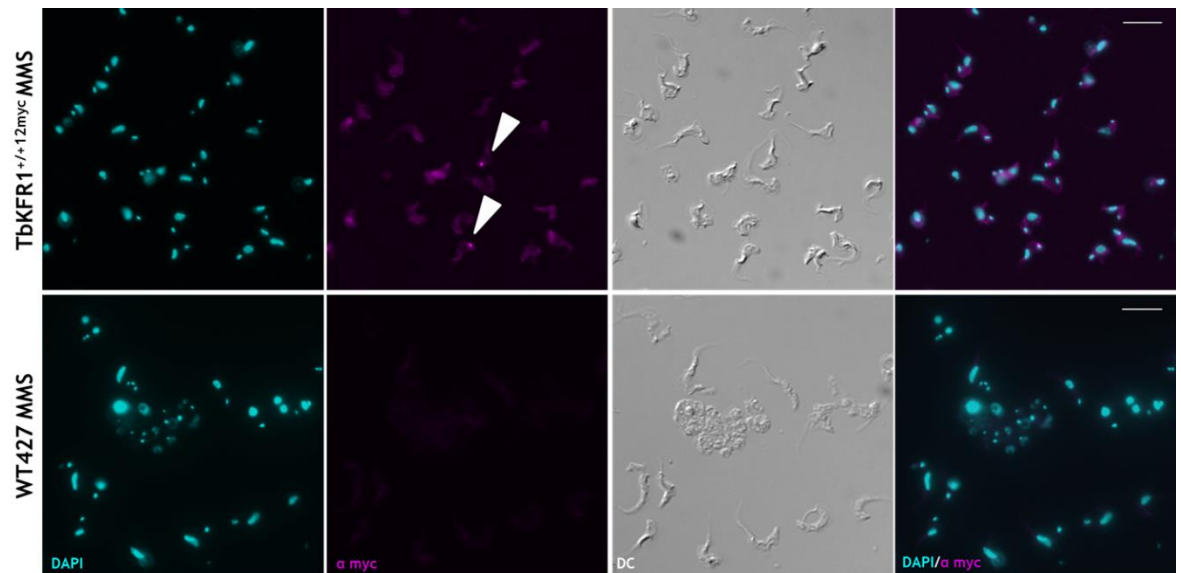


Figure 8-6: TbKFR1 localisation following MMS exposure

WT427 cells (above) and TbKFR1^{+/+12myc} cells (B) were exposed to 18 hrs of either MMS, fixed and stained as per section 2.11.2. Images are representative. Images were captured on an Axioskop2 (Zeiss) and processed as per section 2.11.8 using ImageJ. Scale bar represents 10 μ m.

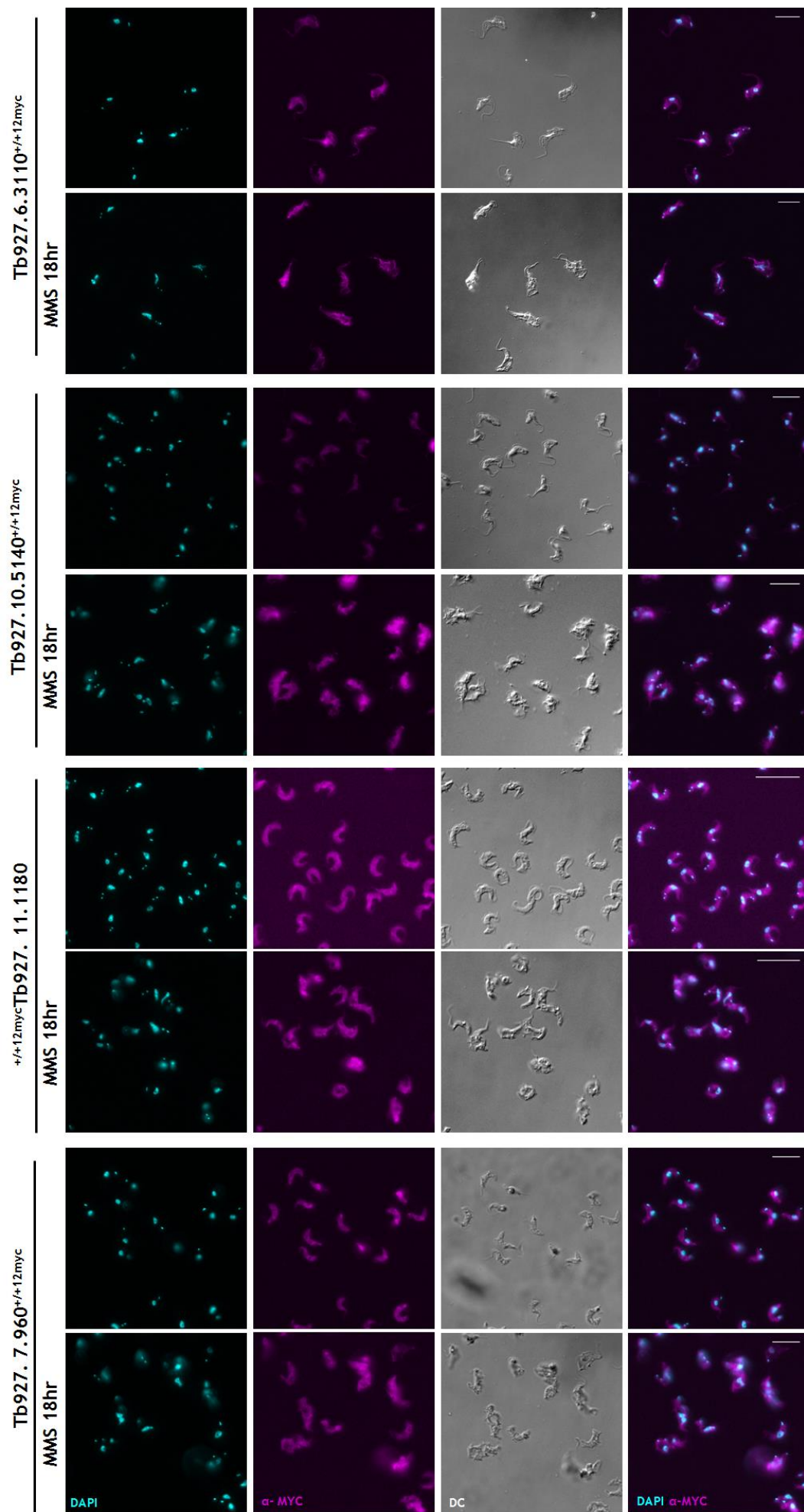


Figure 8-7: Kinome wide candidate localisation in the presence or absence of MMS
Endogenously tagged cells in the absence (above) and presence of 18 hrs exposure to MMS (below) were fixed and stained as per section 2.11.2. Images are representative. Images were captured on an Axioskop2 (Zeiss) and processed as per section 2.11.8 using ImageJ. Scale bar represents 10 μm .

8.3 Chapter 4 appendices

The following section contains the additional material referenced in Chapter 4 (Dissecting the function of TbAUK2 in BSF parasites).

Name of protein	Species	Query Cover (%)	E Value	Identity (%)	Accession Number
Serine/threonine protein kinase	<i>Trypanosoma grayi</i>	88	6e-132	57	XP_009314938.1
Serine/threonine protein kinase	<i>Trypanosoma cruzi</i> CL Brener	79	9e-132	60	XP_804538.1
Serine/threonine protein kinase	<i>Trypanosoma cruzi</i>	79	2e-131	61	EKG04638.1
Serine/threonine protein kinase	<i>Trypanosoma rangeli</i> SC58	81	5e-131	61	ESL10435.1
Serine/threonine protein kinase	<i>Trypanosoma cruzi</i> DM28c	79	7e-131	60	ES567071.1
Serine/threonine protein kinase	<i>Trypanosoma cruzi</i> CL Brener	79	2e-128	60	XP_814913.1
Aurora kinase A isoform b	<i>Mus musculus</i>	75	5e-52	36	NP_001278114.1
Aurora A	<i>Drosophila melanogaster</i>	75	1e-51	36	NP_476749.1
Serine/threonine protein kinase aurora 3	<i>Arabidopsis thaliana</i>	74	3e-50	34	NP_182073.1
Hypothetical protein DDB G0279343	<i>Dictyostelium discoideum</i> AX4	80	3e-50	34	XP_641803.1
Aurora/IPL1-related protein kinase 2	<i>Caenorhabditis elegans</i>	75	6e-49	34	NP_491714.1
Aurora B Kinase Ark1	<i>Schizosaccharomyces pombe</i> 972h-	74	1e-48	35	NP_001018849.1
Aurora kinase A	<i>Danio rerio</i>	76	8e-48	35	NP_001003640.1
Uncharacterised protein LOC100803678	<i>Glycine max</i>	74	6e-46	33	NP_001242251.1
Aurora kinase	<i>Saccharomyces cerevisiae</i> S288c	73	3e-39	31	NP_015115.1
Aurora kinase A isoform a	<i>Mus musculus</i>	77	7e-51	36	NP_035627.1
Aurora kinase C isoform 2	<i>Homo sapiens</i>	76	7e-49	36	NP_001015879.1
Aurora kinase C isoform 3	<i>Homo sapiens</i>	76	8e-49	36	NP_003151.2
Aurora kinase C isoform 1	<i>Homo sapiens</i>	76	1e-48	37	NP_001015878.1
Serine/threonine protein kinase aurora 2	<i>Arabidopsis thaliana</i>	74	2e-47	34	NP_180159.2
Serine/threonine protein kinase aurora 1	<i>Arabidopsis thaliana</i>	74	5e-47	34	NP_195009.1
Aurora kinase B	<i>Mus musculus</i>	76	4e-46	34	NP_035626.1
Serine/threonine protein kinase aurora 1 isoform X2	<i>Glycine mx</i>	74	8e-46	33	XP_00352724.1
Serine/threonine protein kinase aurora 3 isoform X2	<i>Glycine mx</i>	74	9e-46	33	XP_003521942.1
Aurora B	<i>Drosophila melanogaster</i>	84	1e-45	34	NP_477336.1
Aurora kinase C isoform X2	<i>Mus musculus</i>	89	1e-45	31	XP_011248767.1
Aurora kinase C isoform b	<i>Mus musculus</i>	76	2e-45	33	NP_065597.2
Serine/threonine protein kinase aurora 3 isoform X1	<i>Glycine max</i>	76	4e-45	33	XP_006594130.1
Aurora kinase C isoform a	<i>Mus musculus</i>	76	6e-45	33	NP_001074434.1
Aurora kinase B isoform 2	<i>Homo sapiens</i>	81	7e-45	34	NP_001243763.1
Aurora/IPL1 related kinase	<i>Caenorhabditis elegans</i>	76	1e-44	30	NP_505119.1
Serine/threonine protein kinase aurora 1 isoform X1	<i>Glycine max</i>	74	2e-44	33	XP_006578245.1
Aurora kinase B isoform 1	<i>Homo sapiens</i>	81	3e-44	34	NP_004208.2
Aurora kinase B isoform 3	<i>Homo sapiens</i>	76	4e-44	35	NP_001271455.1
Hypothetical protein DDB G0271550	<i>Dictyostelium discoideum</i> AX4	78	2e-43	31	XP_645596.1
Serine/threonine protein kinase aurora 3 like isoform X1	<i>Glycine max</i>	74	1e-41	31	XP_006576401.1
Calcium/calmodulin dependant protein kinase IG isoform X1	<i>Danio rerio</i>	80	1e-39	30	XP_005174189.1
Calcium/calmodulin dependant protein kinase IG	<i>Danio rerio</i>	80	1e-39	30	NP_957123.1
Serine/threonine protein kinase aurora 3 isoform X2	<i>Glycine max</i>	65	2e-39	34	XP_014621005.1
Calcium/calmodulin dependent protein kinase IG isoform X2	<i>Danio rerio</i>	80	3e-39	30	XP_005174188.2
Calcium/calmodulin dependent protein kinase type 1	<i>Caenorhabditis elegans</i>	81	4e-39	32	NP_500139.1
Protein kinase	<i>Leishmania donovani</i>	82	4e-39	31	XP_003862154.1
Serine/threonine protein kinase	<i>Leishmania donovani</i>	81	7e-39	31	XP_003861575.1
Calcium/calmodulin dependent protein	<i>Homo sapiens</i>	79	2e-38	32	NP_065130.1

Table 8-4: Additional ‘hits’ retrieved from the SmartBLAST analysis
Additional ‘hits’ retrieved from the SmartBLAST analysis using the SmartBLAST feature of the NCBI BLAST platform (<http://blast.ncbi.nlm.nih.gov/Blast.cgi>). Accession numbers (as annotated in the NCBI database; <http://www.ncbi.nlm.nih.gov/>) are presented in the far right column.

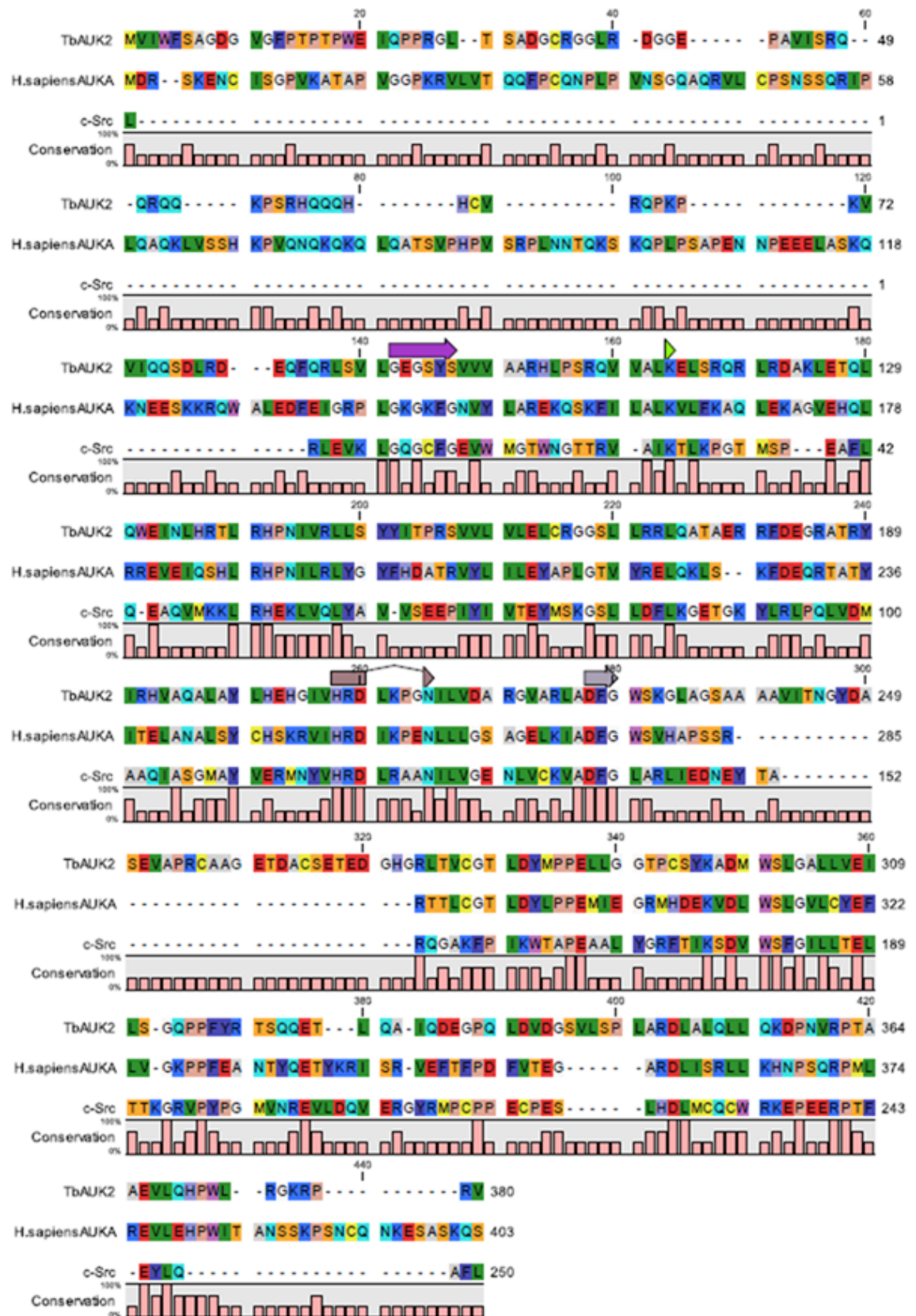


Figure 8-8: Protein sequence alignments between TbAUK2, AUKA and c-Src
The protein sequences of TbAUK2 (*Trypanosoma brucei*: TbAUK2 on the diagram), AUKA from *Homo sapiens* (*H. sapiens* AUKA) and c-Src were aligned in CLC Genomics Workbench 7. The purple arrow indicated the GxGxxG sequence motif, the brown arrow the HRD motif and the grey arrow the DFG motif. The Tb927.3.3920 sequence was retrieved from TriTrypDB, v28. The other sequences were retrieved from the NCBI database. The

consensus sequence is shown below the corresponding alignment. Coloured using Rasmol colour palette in CLC Genomics Workbench 7. Accession numbers: *T. brucei* (Tb927.3.3920; TREU 927), *H. sapiens* (NP_003591.2) and c-Src (GenBank ID 125711).

Figure 8-9: Protein sequence alignments between the *T. brucei* aurora kinases
The protein sequences of TbAUK2 (Tb927.3.3920), TbAUK1 (Tb927.11.8220) and TbAUK3 (Tb927.9.1670) were aligned in CLC Genomics Workbench 7. The sequences were retrieved from TriTrypDB, v28. The consensus sequence is shown below the corresponding alignment. Coloured using Rasmol colour palette in CLC Genomics Workbench 7. Accession numbers are as shown on the diagram.

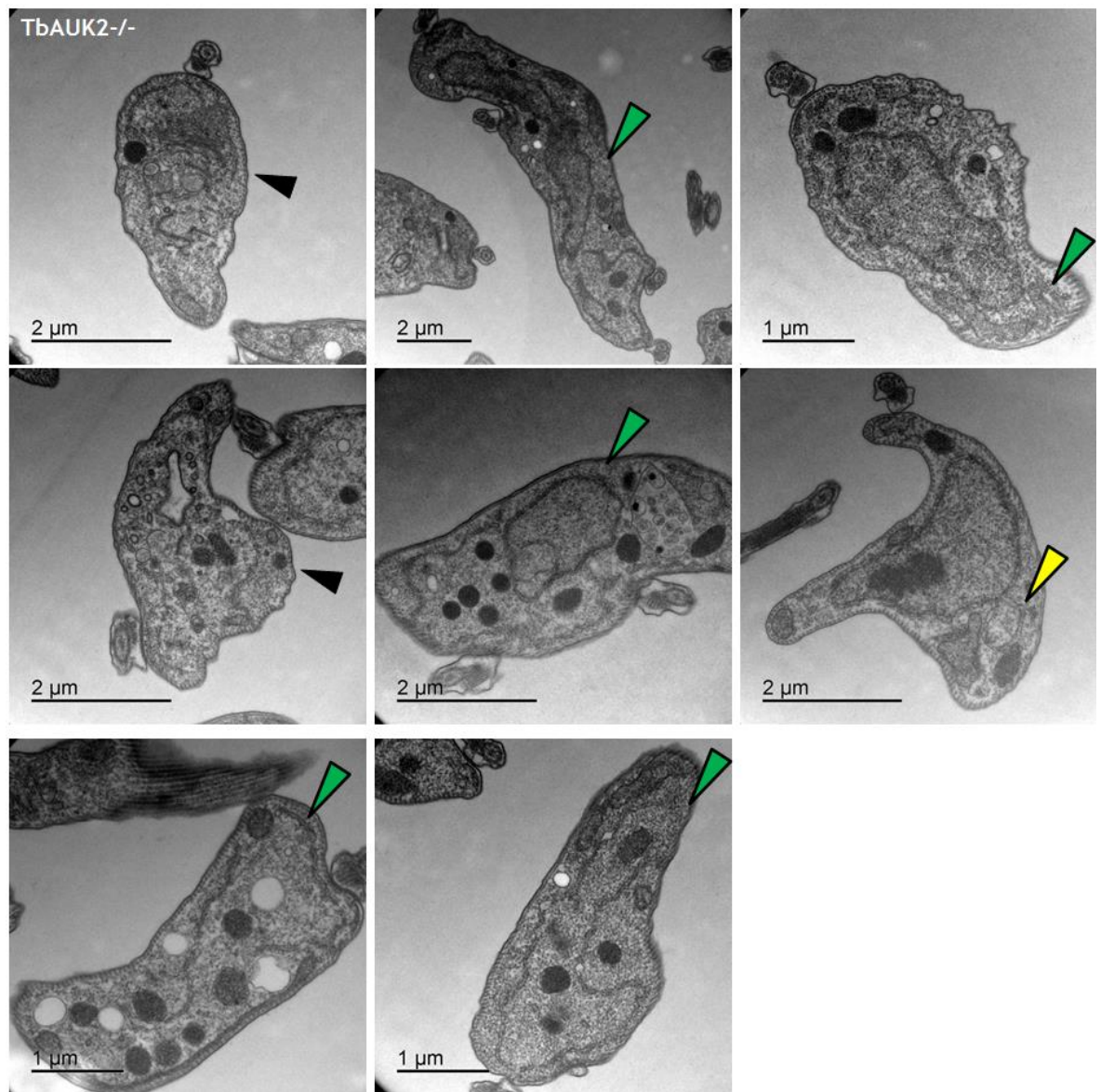


Figure 8-10: Additional examples of nuclei imaged by TEM from TbAUK2 $-/-$ cells
 Additional examples of nuclei from TbAUK2 $-/-$ CL2 cells. Scale bar sizes are indicated on each image. In all examples, large, electron dense vacuoles can be seen within the cytoplasm of the cell. Additionally, the nucleus of the cell appears abnormal. The black arrows indicate cells with an 'unclear phenotype'. The green arrows indicate cells with abnormal arrangement of the nucleus including additional nuclear membranes. The yellow arrow indicates a cell with a nuclear 'bleb'. These cells could not clearly be categorised. Further processing and imaging of the samples was kindly conducted by L. Lemgruber Soares. Images were captured on a Tecnai T20 transmission electron microscope as per section 2.11.7.2.

For all raw cell counts (excluding growth curve values), see files labelled Cellcountsmasterspreadsheet.xls presented in the accompanying CD.

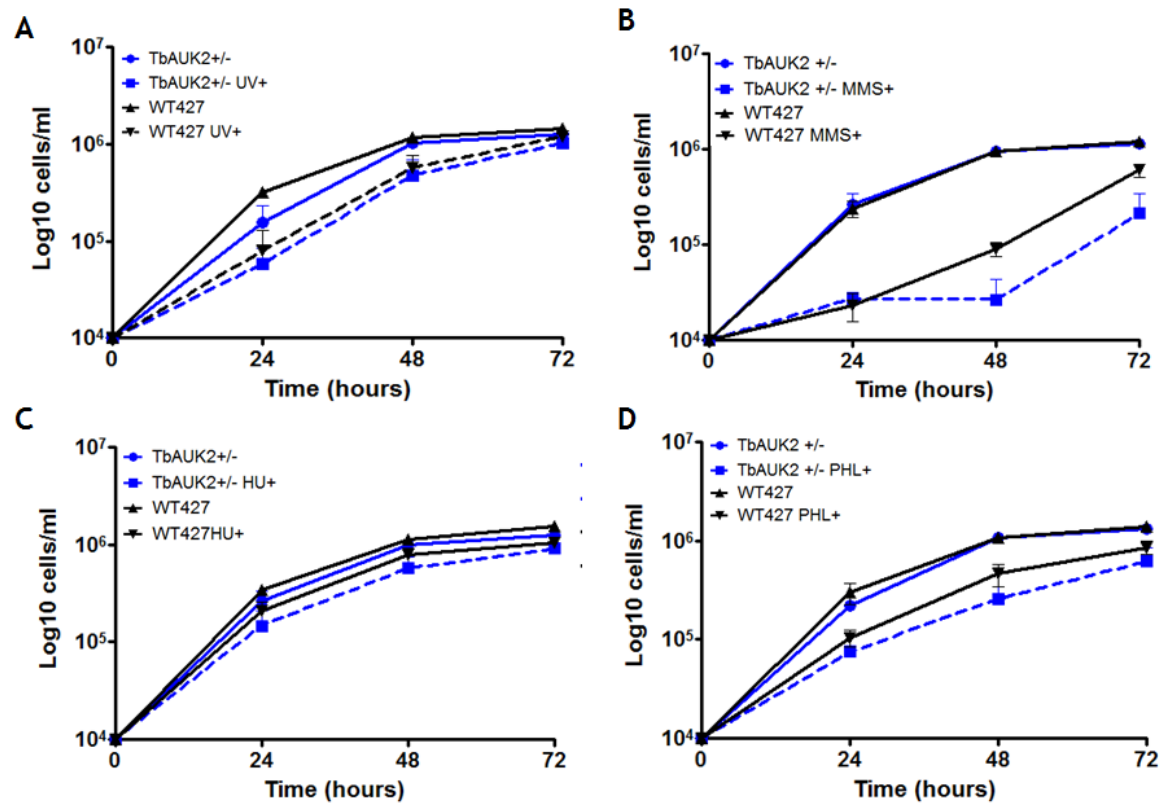


Figure 8-11: *In vitro* growth of TbAUK2 +/- cell lines following treatment with DNA damaging agents

Growth analysis of TbAUK2 +/- under a variety of genotoxic stress sources as per section 2.8.1. UV (A; 1500 J/m²), MMS (B; 0.0003%), HU (C; 0.06 mM), PHL (D; 0.1 μ g/ml). The data is plotted on a logarithmic scale. The error bars represent \pm SEM, n=3.

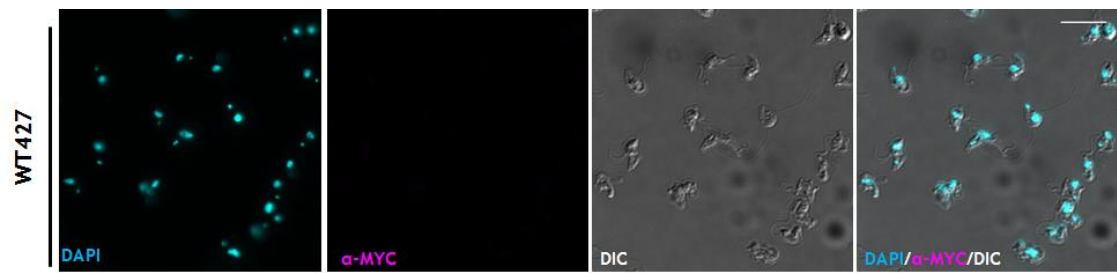


Figure 8-12: Anti myc antiserum does not bind non-specifically to WT427 cells
 Representative images of WT427 cells fixed and stained with α myc to control for non-specific antiserum binding (green) as per section 2.11.2. The nDNA and kDNA were stained with DAPI (blue). The cell body was visualised by DIC imaging. Images were captured on an Axioskop 2 and processed in ImageJ as per section 2.11.8. Scale bars = 10 μ m.

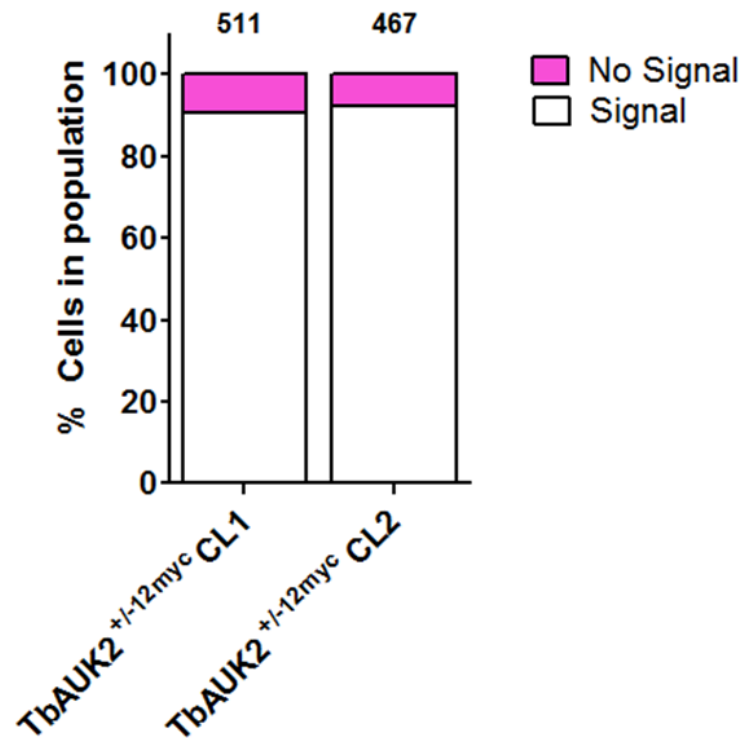


Figure 8-13: TbAUK2 fails to localise in a population of cells

TbAUK2^{+/-12myc} cells were fixed and stained as per section 2.11.2. Images were captured on an Axioskop2 and the background subtracted in ImageJ as described in section 2.11.8. Cells were scored based on whether the nuclear localisation of TbAUK2 could be observed. The number of cells counted for each clone is indicated above the corresponding bar on the graph above. This experiment was performed once.

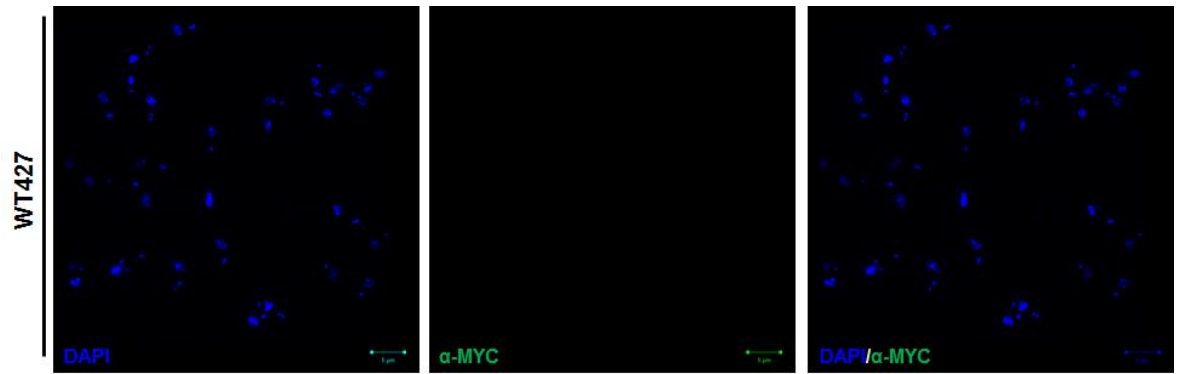


Figure 8-14: Super resolution imaging of WT427 cells stained with anti myc antiserum
 Super resolution images of WT 427 cells stained with anti myc antiserum. Cells were fixed and stained as per section 2.11.2. Scale bar = 5 μm . (B) 3D reconstructions of TbAUK2 localisation. The images were captured on an Elyra (Zeiss) super resolution microscope as per section 2.11.8. The images were captured and prepared under the supervision of L. Lemgruber Soares.

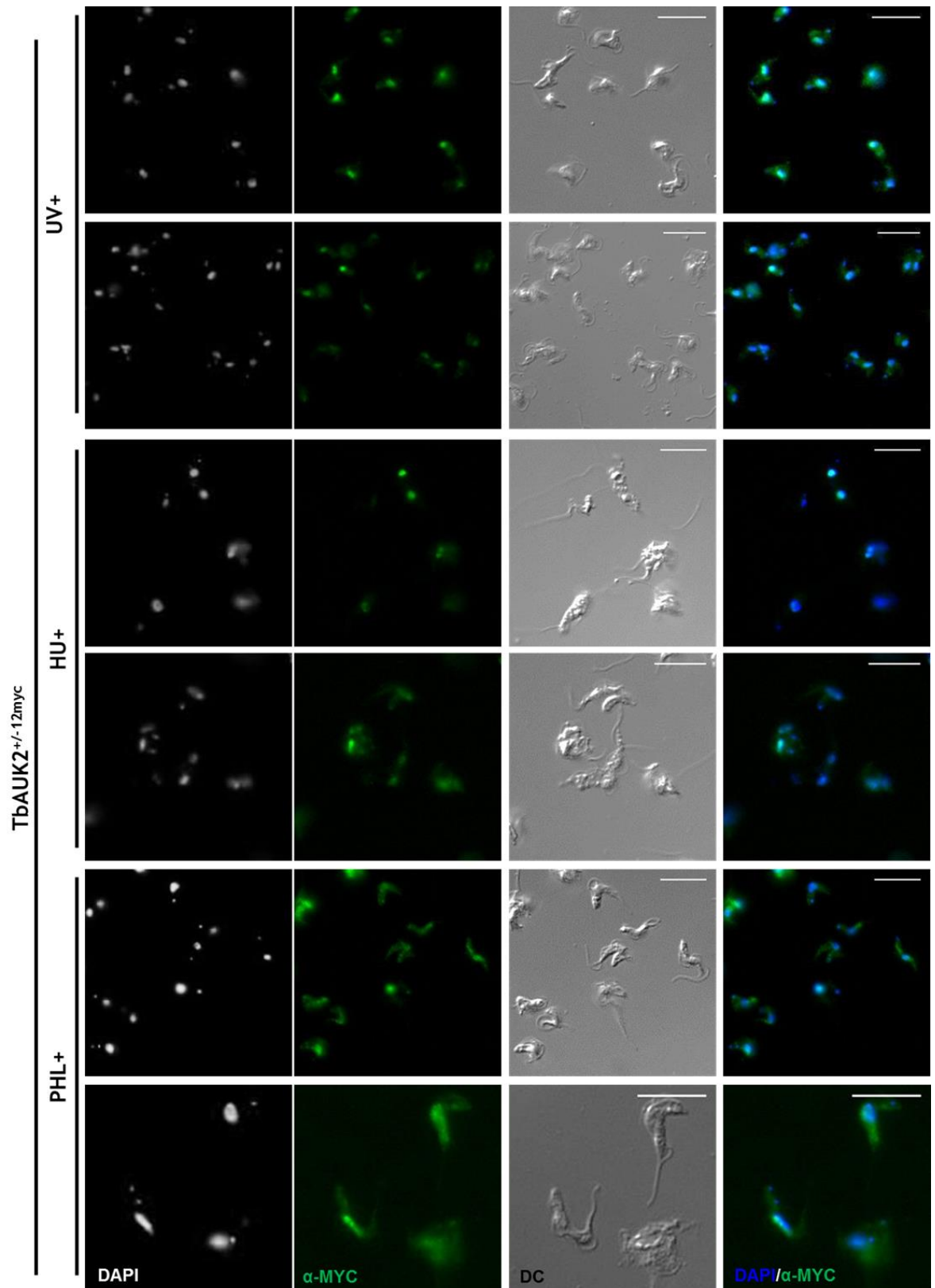


Figure 8-15: Localisation of TbAUK2 after HU, UV and PHL exposure

The cells were exposed to UV (1500 J/m^2), HU (0.06 mM) and PHL (0.1 $\mu\text{g/ml}$) for 18 hrs before fixation and IF analysis (performed as per section 2.8.3 and 2.11.2). The myc tag (green) was visualised using $\alpha \text{ myc::FITC}$ conjugate antibody. The nDNA and kDNA were stained with DAPI (White). Scale bar = 10 μm . Images were captured on an Axioskope 2 (as per section 2.11.8). Images are of $\text{TbAUK2}^{+/-12\text{myc}}$ CL1.

For all raw mass spectroscopy data, see Excel file labelled
MSdataTb6560andTbAUK22016.xls presented in the accompanying CD.

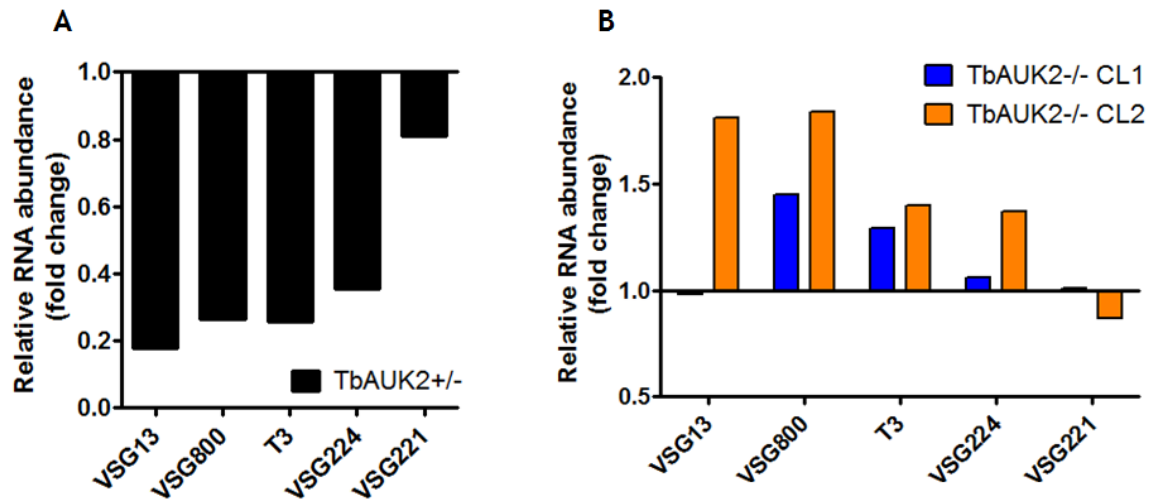


Figure 8-16: Loss of TbAUK2 is not associated with expression of silent VSG RNA transcripts

The levels of gene expression were assessed by qRT-PCR from TbAUK2+/- cells (A) and TbAUK2-/- CL1 and CL2 cells (B). The CT values for each sample were generated by averaging the CT values across the triplicate technical repeats, n=1. The relative fold change for each VSG examined was then calculated by calculating the $\Delta\Delta CT$ value for each normalised to the endogenous control (for this experiment actin was used in WT427 cells). The levels of RNA from WT427 cells were set to 1 (represented by the black line). The following VSGs were examined: VSG13 (telo 59 and 51; BES 17), VSG221 (telo 40; BES1), VSG224 (telo65 and 153; BES7), VSGT3 (telo 3 and 28; BES4) and VSG800 (telo 98; BES5). VSG13 and VSGT3 are located on intermediate chromosomes. VSG224, VSG221 and VSG800 are located on megabase chromosomes. Named as detailed in Hertz-Fowler et al. 2008.

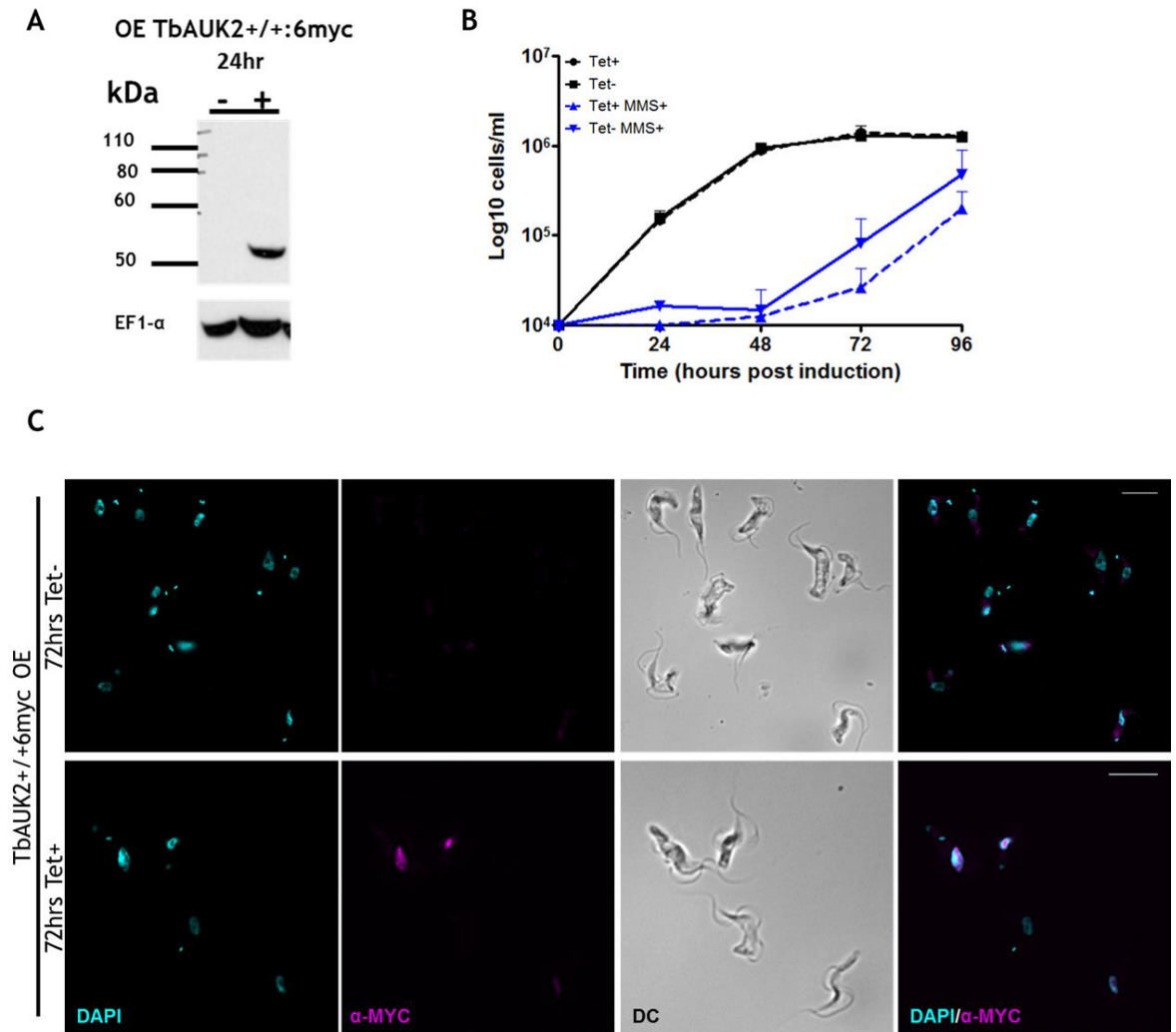


Figure 8-17: Overexpression of TbAUK2 does not affect cellular proliferation or increase sensitivity to MMS

One clone was induced for 24 hrs with $1 \mu\text{g/ml}^{-1}$ tetracycline and whole cell lysates prepared from induced and non-induced cells. Western blot analysis (A) was performed (section 2.12.1) to examine for expression of the endogenously tagged overexpressed TbAUK2 (49.3 kDa in total). Western blot analysis was performed on whole cell lysates. The membrane was probed with α myc antibody. EF1 α was used as a loading control. (B) Growth analysis of TbAUK2 overexpressing cell lines was monitored in the presence and absence of MMS (0.0003 % v/v) following induction as described in (A). The data is plotted on a logarithmic scale. The error bars represent \pm SEM, $n=2$. (C) Overexpressed TbAUK2 localises to the nucleus of BSF cells. Representative images of cells at 72 hrs post tetracycline induction. The cells were fixed and stained with α myc to visualise the myc tagged TbAUK2 (magenta). The nDNA and kDNA were stained with DAPI (cyan). The cell body was visualised by DC imaging. Images were captured on a DeltaVision microscope and processed in ImageJ as per section 2.11.8. Scale bars = 10 μm .

8.4 Chapter 5 appendices

The following section contains the additional material referenced in Chapter 5 (Tb6560 is a pseudokinase that acts in BSF endocytosis).

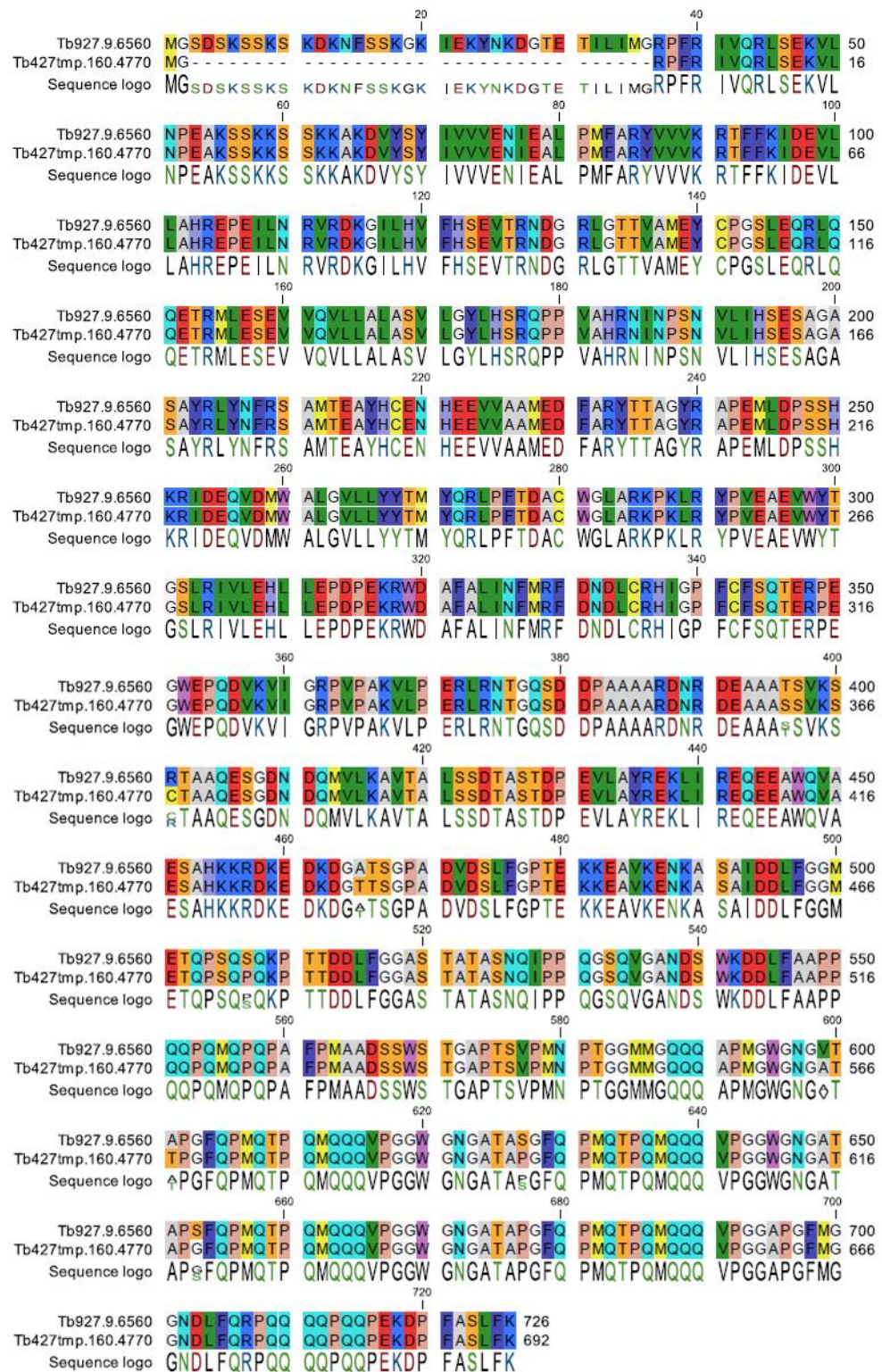
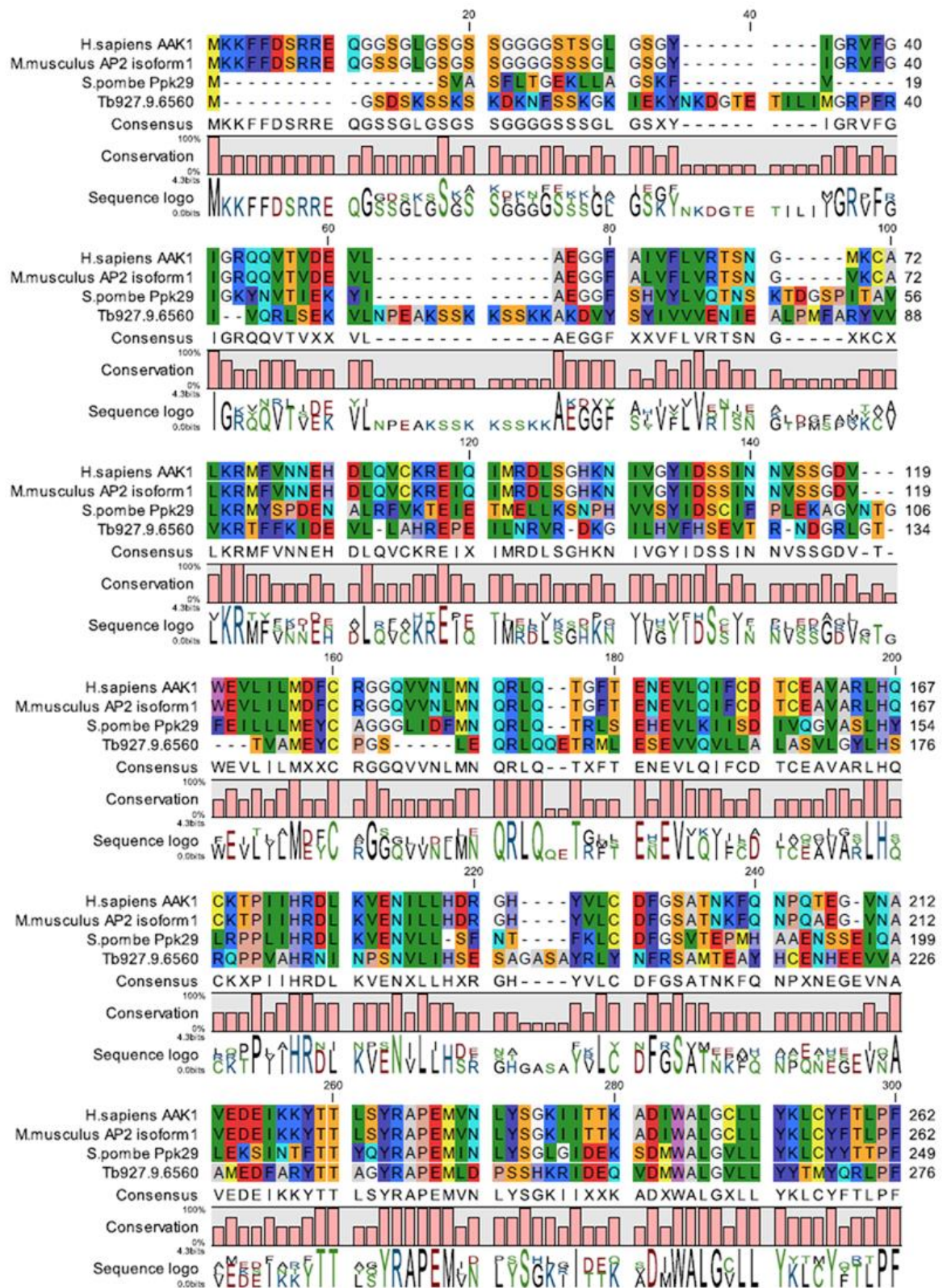
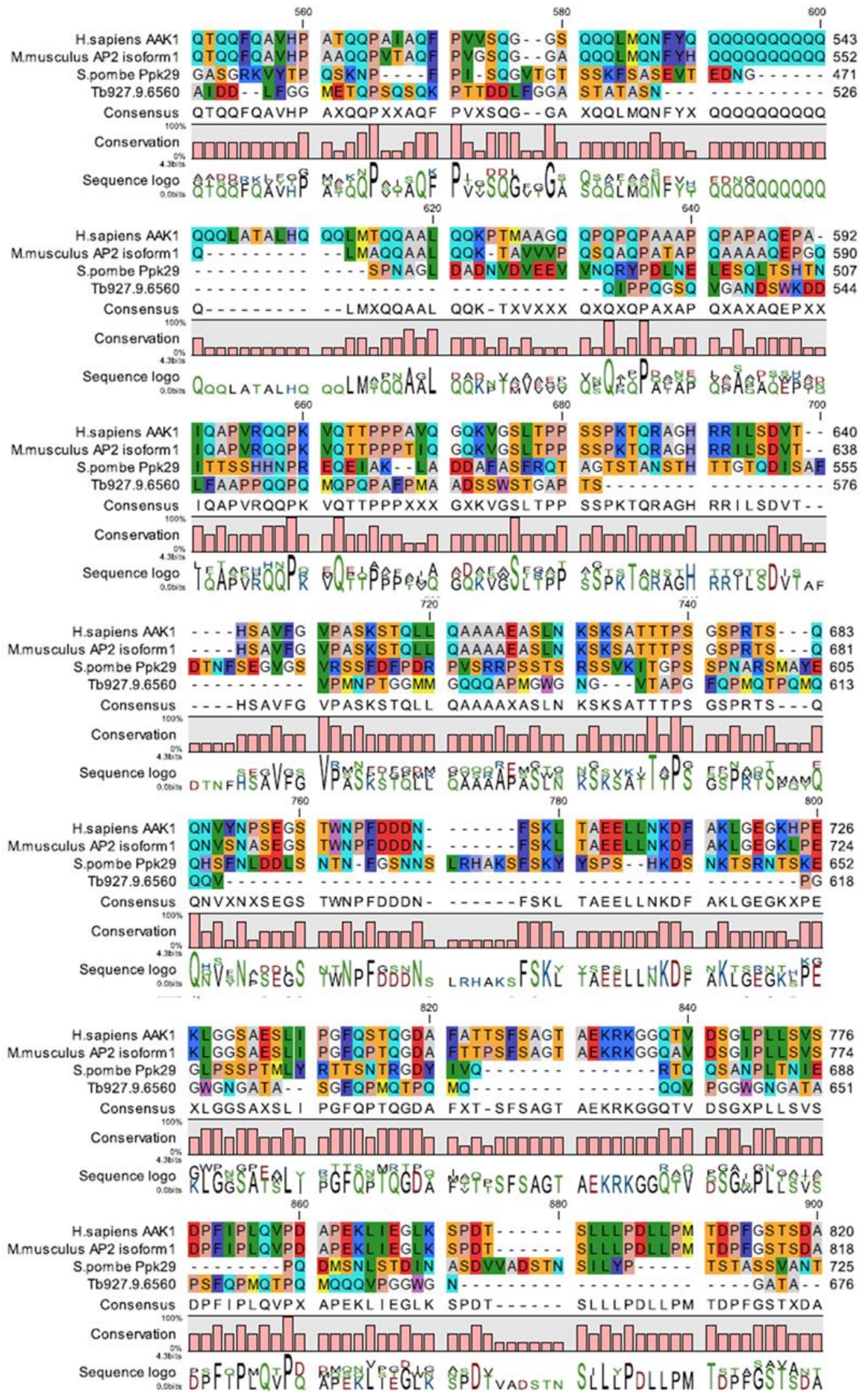


Figure 8-18: Amino acid sequence alignments between the Tb6560 TREU 927 and Lister 427 sequences

The protein sequences of Tb6560 from the TREU 927 and the Lister 427 genome (retrieved from TriTrypDB, v28) were aligned in CLC Genomics Workbench 7. The consensus sequence is shown below the corresponding alignment. Coloured using Rasmol colour palette in CLC Genomics Workbench 7. Accession numbers are labelled on the alignment.





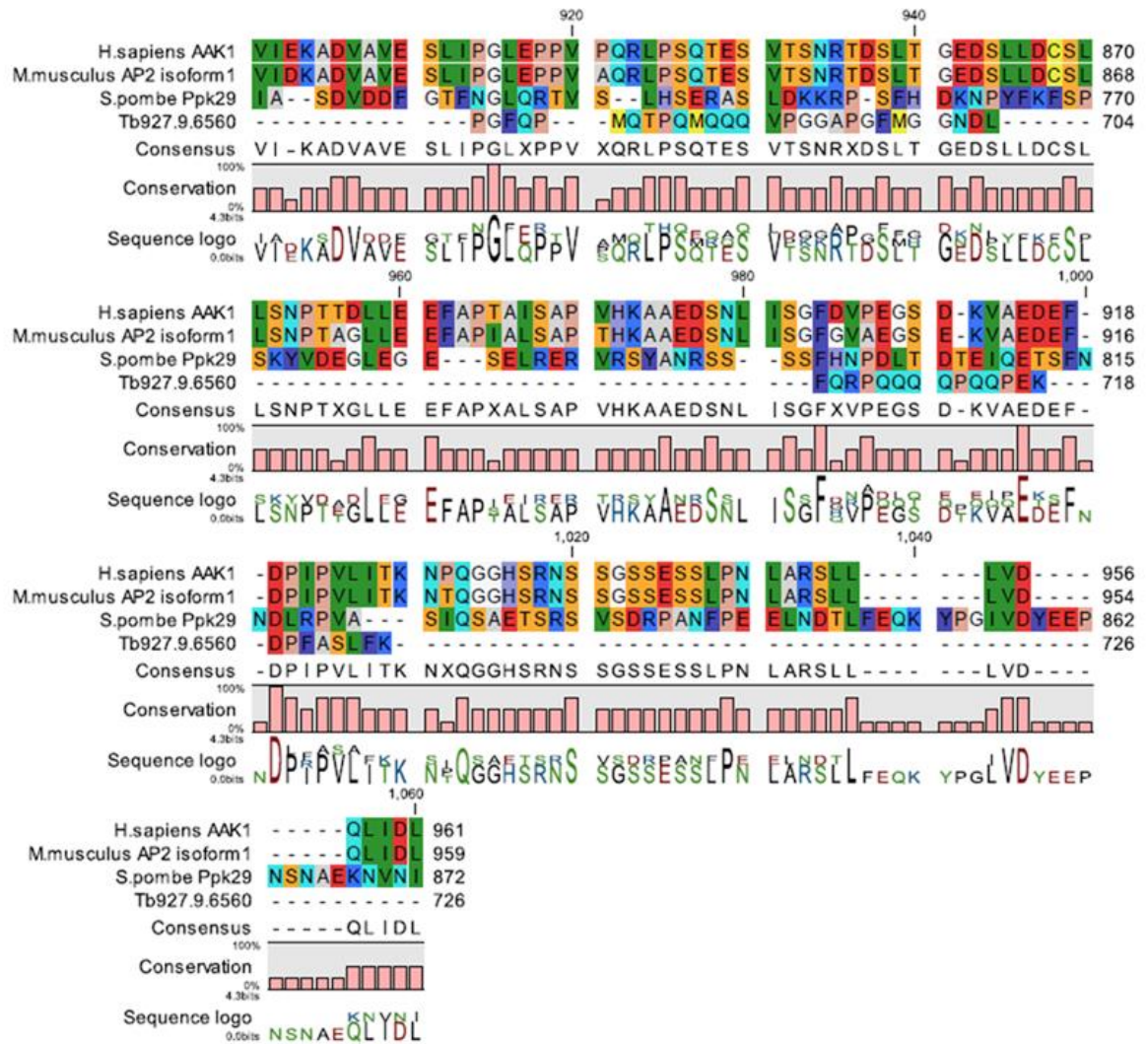
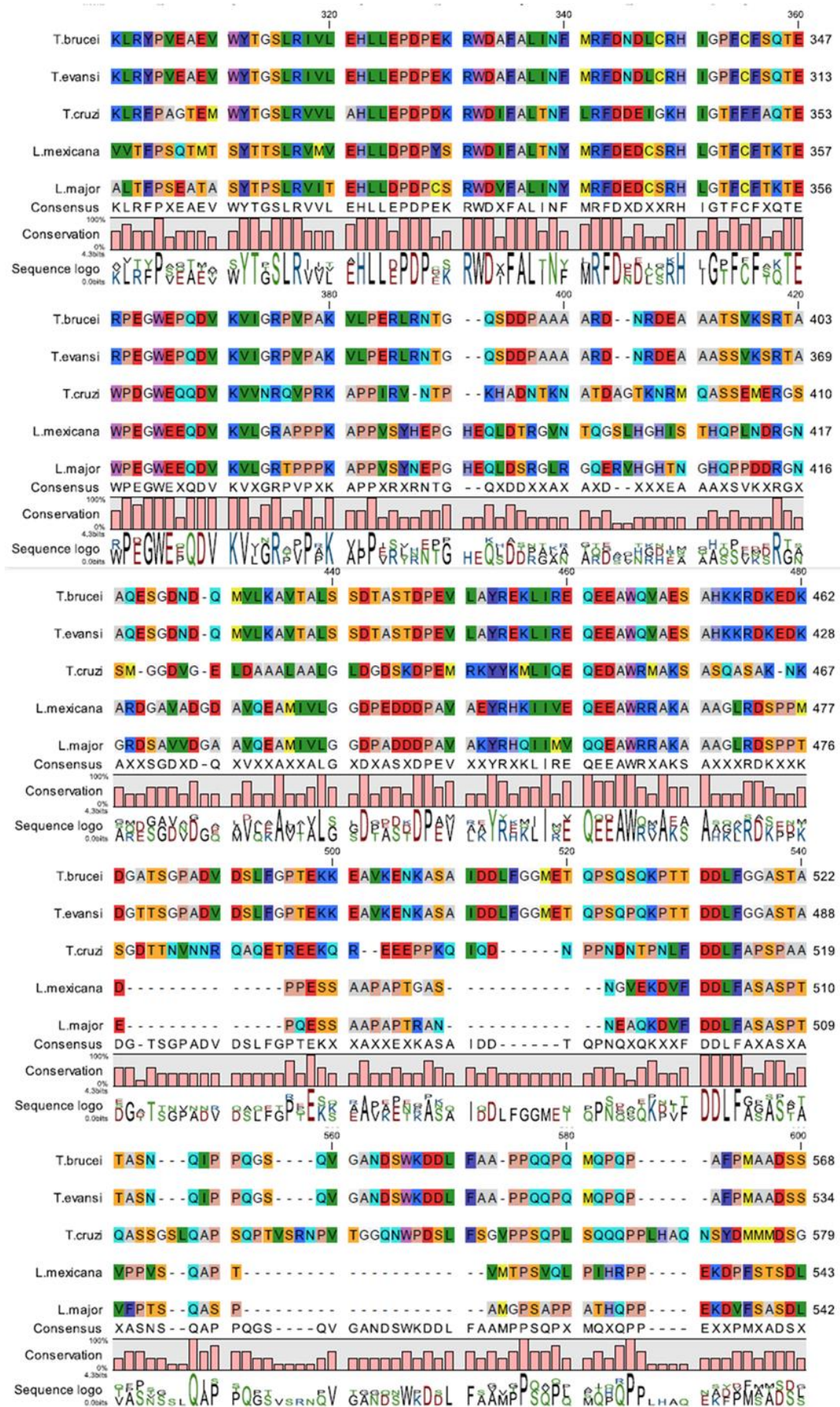


Figure 8-19: Full amino acid sequence alignments between the Tb6560 TREU 927 sequence and the putative homologues in other organisms

The protein sequences of Tb6560 (*Trypanosoma brucei*: Tb927.9.6560 on the diagram) and the putative homologues from *Mus musculus* (*M. musculus*), *Schizosaccharomyces pombe* (*S. pombe*), and *Homo sapiens* (*H. sapiens*) were aligned in CLC Genomics Workbench 7. The Tb927.9.6560 sequence was retrieved from TriTrypDB, v28. The other sequences were retrieved from the NCBI database. The consensus sequence is shown below the corresponding alignment. Coloured using Rasmol colour palette in CLC Genomics Workbench 7. Accession numbers: *T. brucei* (Tb927.9.6560; TREU 927), *M. musculus* (NP_001035195.1), *S. pombe* (NP_596027.1; 972h-), *H. sapiens* (NP_055726.3).



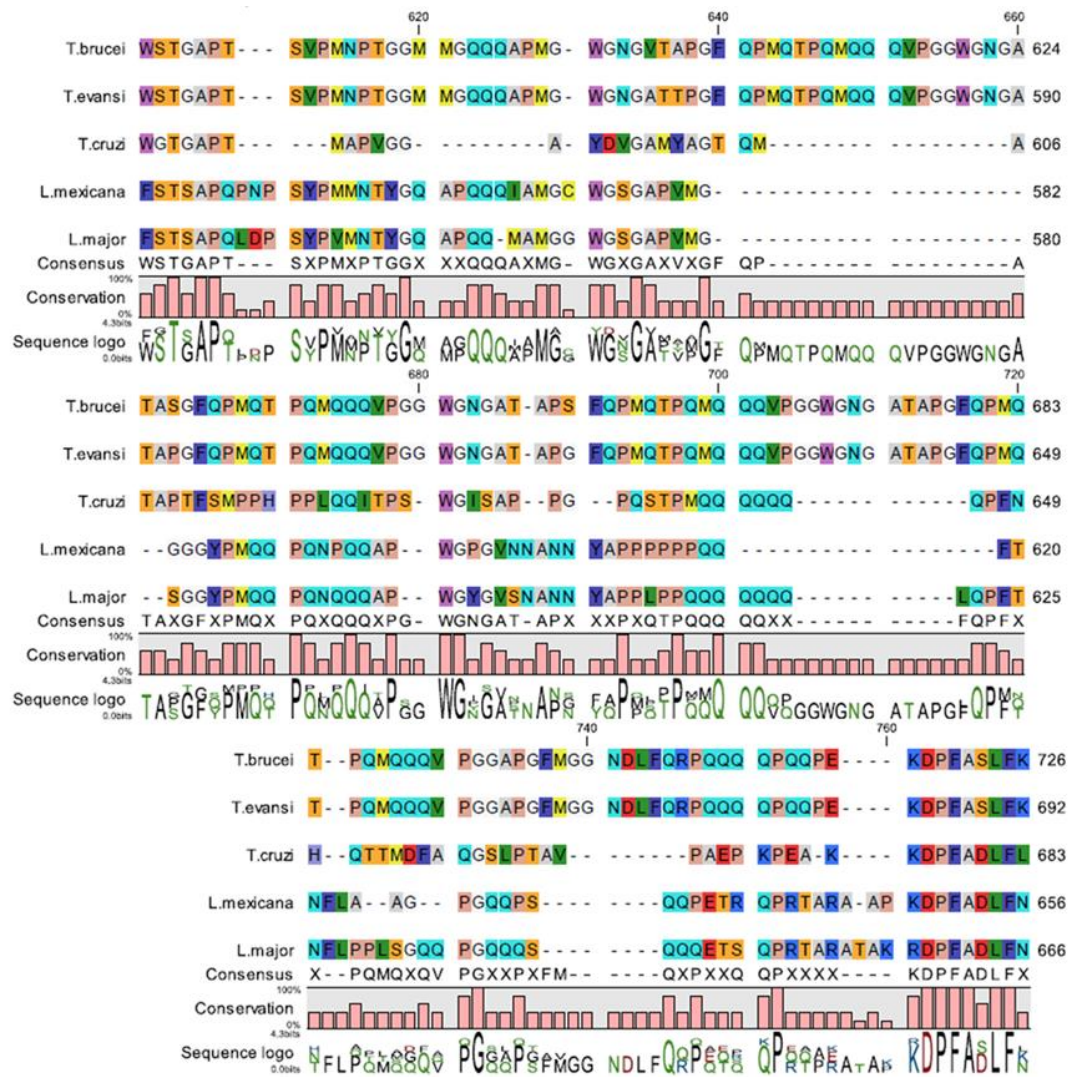


Figure 8-20: Amino acid sequence alignments between the Tb6560 TREU 927 sequence and the putative orthologues in other kinetoplastid parasites
The protein sequences of Tb6560 (*Trypanosoma brucei*; *T. brucei* on the diagram) and the putative kinetoplastid orthologues from *Leishmania major* (*L. major*), *Leishmania mexicana* (*L. mexicana*), *Trypanosoma evansi* (*T. evansi*) and *Trypanosoma cruzi* (*T. cruzi*; retrieved from TriTrypDB, v28) were aligned in CLC Genomics Workbench 7. The consensus sequence is shown below the corresponding alignment. Coloured using Rasmol colour palette in CLC Genomics Workbench 7. Accession numbers: *T. brucei* (Tb927.9.6560; TREU 927), *T. evansi* (TevSTIB805.9.4690; strain STIB 805), *T. cruzi* (TcCLB.504883.10; CL Brener Esmeraldo-like), *L. mexicana* (LmxM.15.0770; MHOM/GT/2001/U1103), *L. major* (LmjF.15.0770; Friedlin). No clear GxGxxGG position could be established based on the sequences above. As such it is not marked on the alignment. The following arrows highlight the potential positions of the following motifs; pale green arrow = "HRD", dark green arrow = "DFG" and blue arrow = "APE".

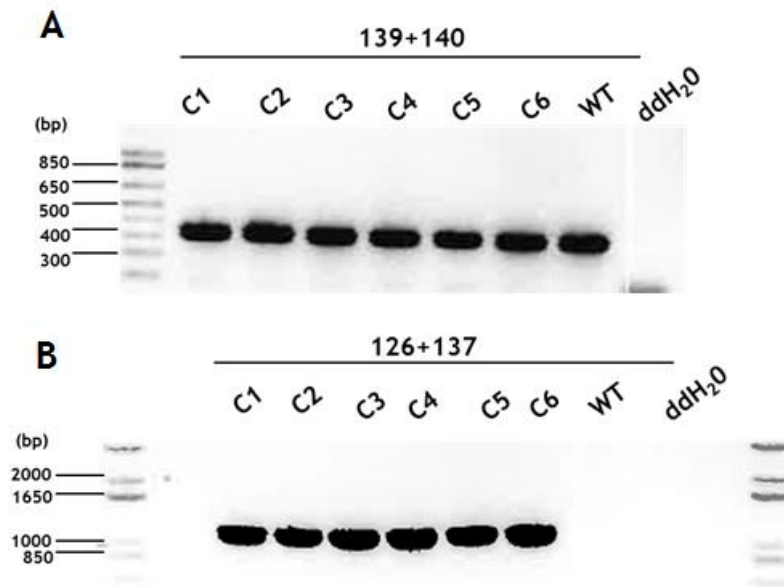


Figure 8-21: PCR analysis of putative Tb6560 heterozygote (+/-) clones

Agarose gels of diagnostic integration PCRs, which were performed using the primer pairs detailed in Figure 5-6 (section 5.3.2; chapter 5) testing for the presence of the intact ORF (A) and the integration of BSD (B) using gDNA from six putative (+/-) clones (CL1 to CL6), wild type (WT) cells, or using double distilled water (ddH₂O) as a negative control. All PCRs were performed on the same gDNA samples. For each gel, size markers are shown (bp). Diagnostic primers used (black arrows) and the corresponding primer sequences are available in Table 2-3.

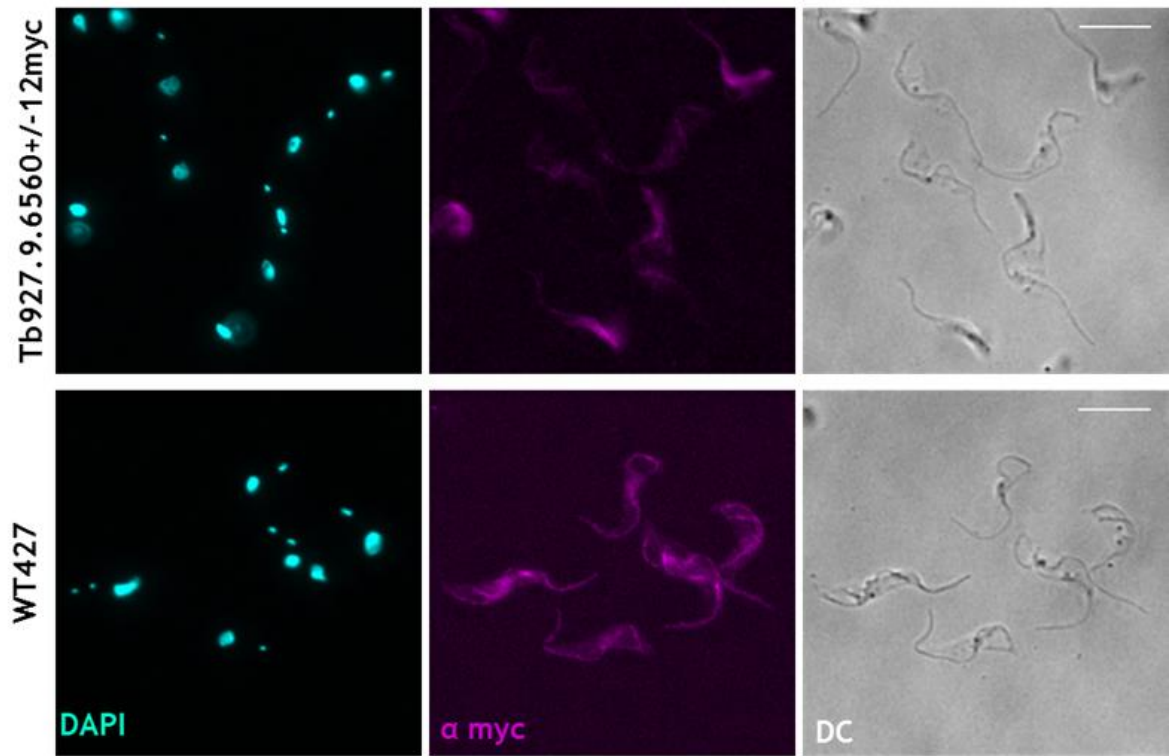


Figure 8-22: Tb6560 localisation following cytoskeleton extraction
 Cytoskeletal preparations of WT427 cells (below) and Tb6560^{+/-12myc} cells (above) were prepared, fixed and stained as per section 2.11.2. Representative images are shown and were captured on an Axioskop2 (Zeiss) and processed as per section 2.11.8 using ImageJ. The myc epitope was visualised using α myc antiserum. Scale bar represents 10 μm. Images shown are from Tb6560^{+/-12myc} CL1.

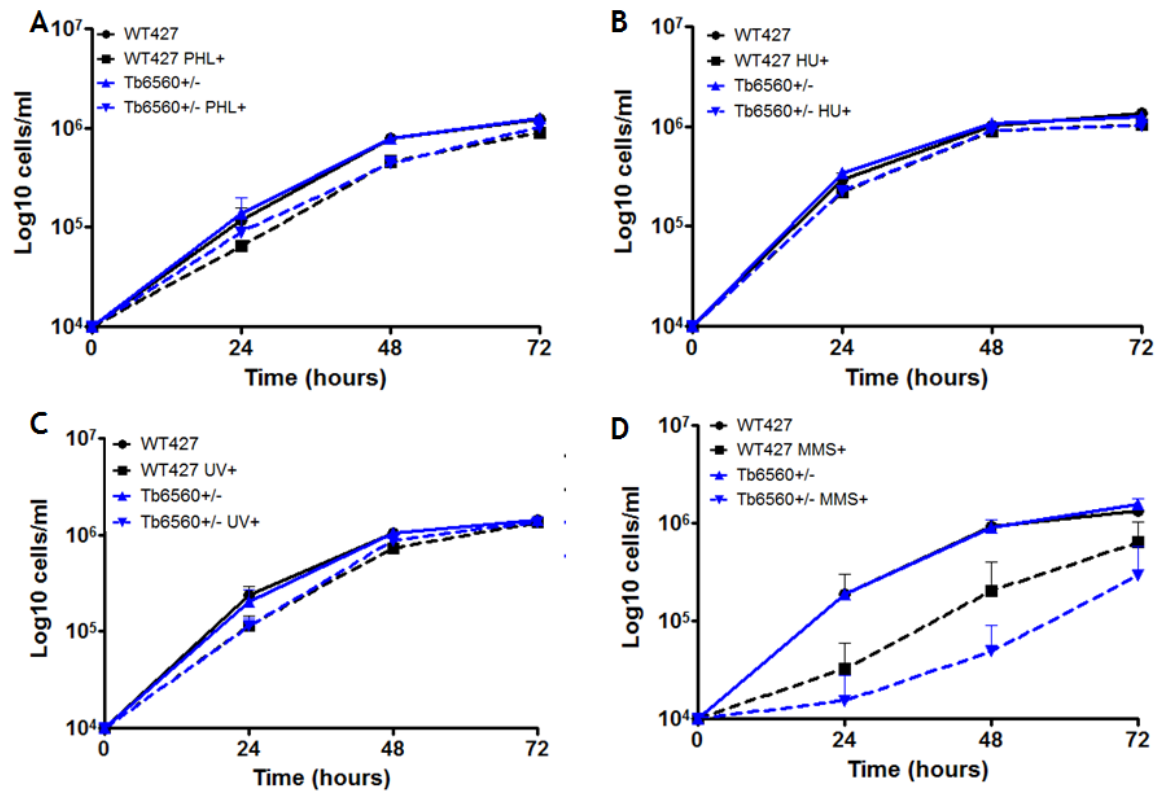


Figure 8-23: *In vitro* growth analysis of *Tb6560*^{+/-} cells under genotoxic stress
 Growth analysis of *Tb6560*^{+/-} (blue lines) in the presence (dashed lines) or absence (solid lines) of a variety of genotoxic stress conditions (as per section 2.8.2): MMS (D; 0.0003%), UV (C; 1500 J/m²), PHL (A; 0.1 $\mu\text{g/ml}^{-1}$) and HU (B; 0.06 mM). Black lines depict growth of the WT cells. Error bars represent \pm SEM; n=3 for A and C or n=3 for B and D. *Tb6560*^{+/-} clone used: Clone C1.

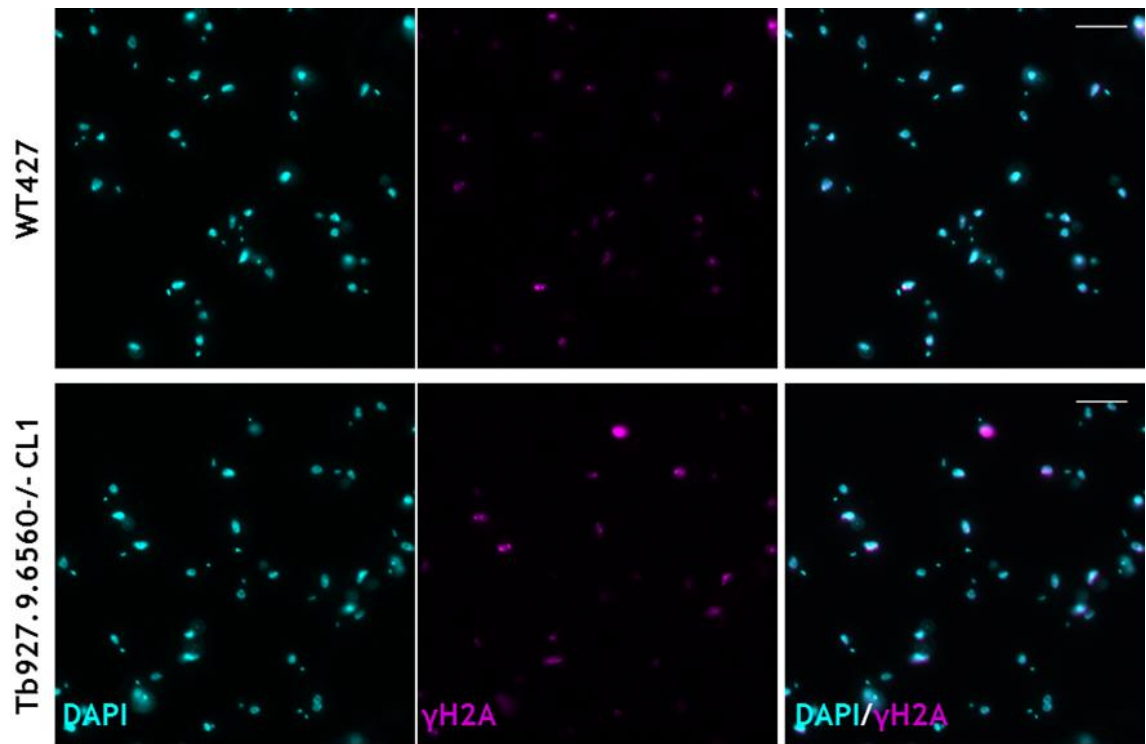


Figure 8-24: Expression of γ H2A in WT and Tb6560 null mutant cells
 WT427 cells (above) and Tb6560^{+/-12myc} cells (below) were fixed and stained as per section 2.11.2. Representative images are shown and were captured on an Axioskop2 (Zeiss) and processed as per section 2.11.8 using ImageJ. γ H2A was detected using α γ H2A antiserum. Scale bar represents 10 μ m. Images shown are from Tb6560^{+/-12myc} CL1.

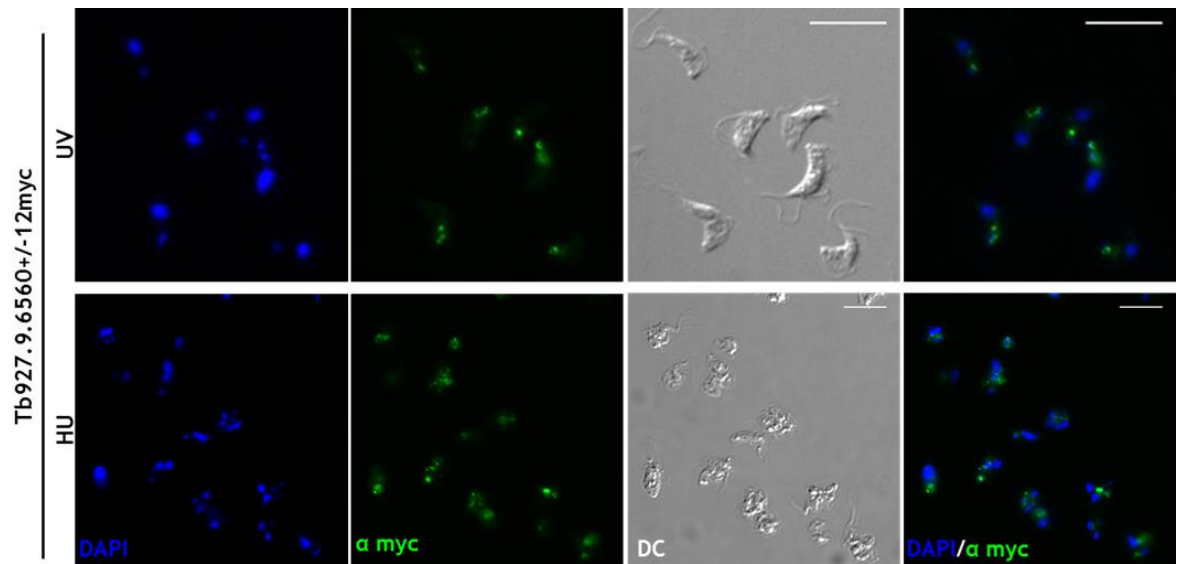


Figure 8-25: Tb6560 localisation following DNA damage exposure
 Tb6560^{+/-12myc} cells were exposed to UV (1500 J/m²) or HU (0.006 mM) for 18 hrs (section 2.8.3), fixed and stained as per section 2.11.2. Representative images are shown and were captured on an Axioskop2 (Zeiss) and processed as per section 2.11.8 using ImageJ. Scale bar represents 10 µm. Images shown are from Tb6560^{+/-12myc} CL1.

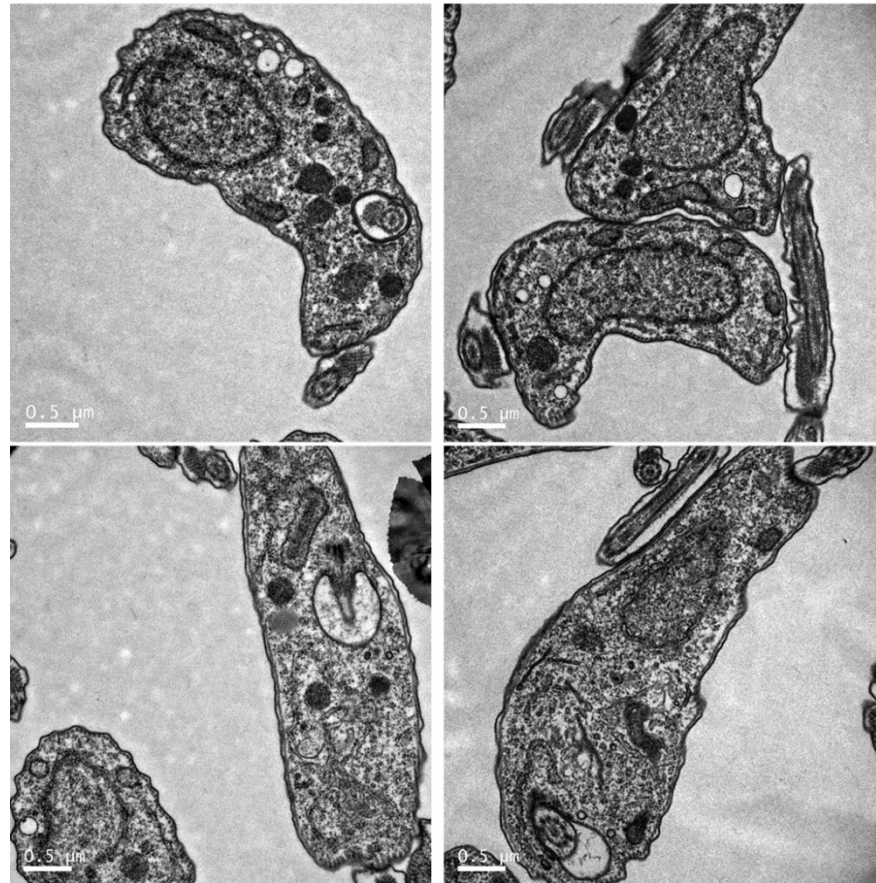
Tb6560^{+/-}

Figure 8-26: Tb6560^{+/-} cells images by TEM

Representative images of the Tb6560^{+/-} cell line. Cells were fixed as per section 2.11.7.2 and imaged on a Tecnai T20 transmission electron microscope using TEM. Images were processed in ImageJ and Adobe Photoshop (by L. Lemgruber-Soares). Scale bars are as annotated on the images (all 0.5 μm).

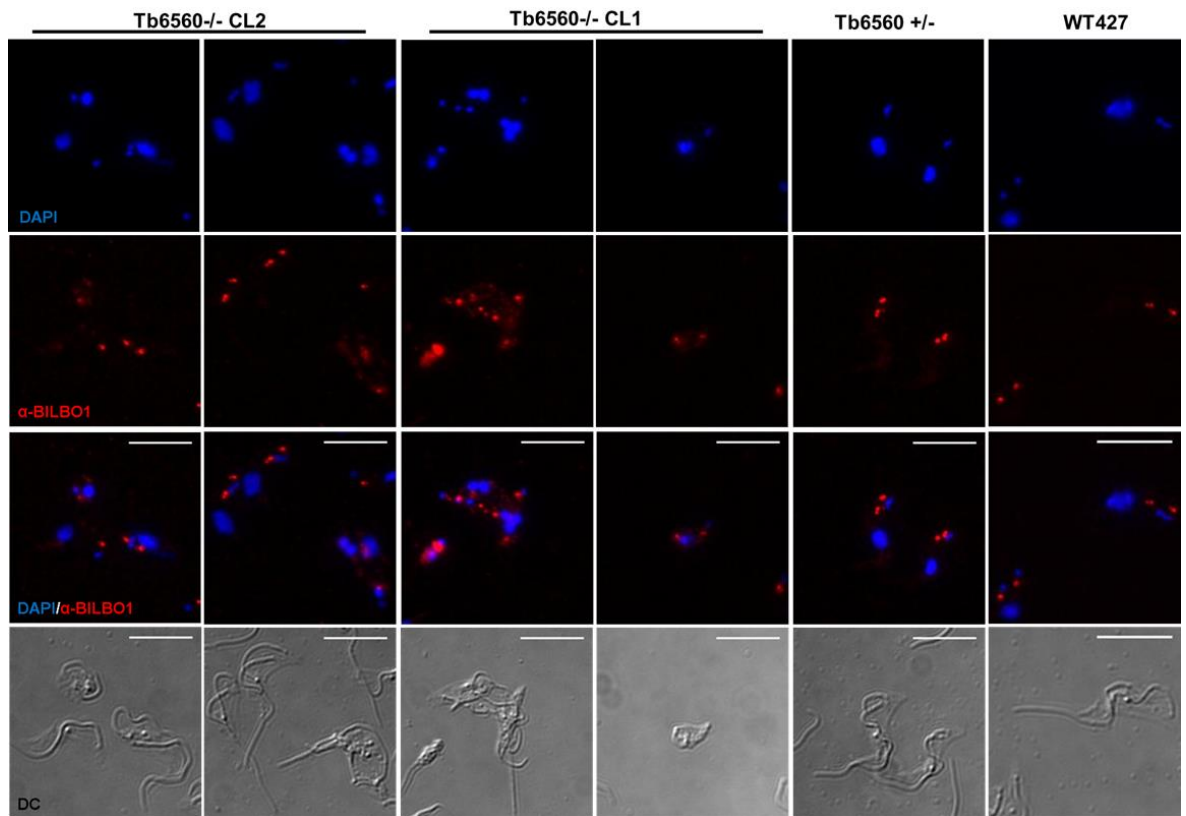


Figure 8-27: TbBILBO-1 localisation in Tb6560 null mutant cell lines
 Cytoskeletal preparations of Tb6560-/- cells (CL1 and CL2), WT cells and Tb6560+/- cells were fixed and stained as per section 2.11.5. Representative images are shown and were captured on an Axioskop2 (Zeiss) and processed as per section 2.11.8 using ImageJ. Scale bar represents 10 μ m.

For the FIB/SEM video referred to in chapter 5 (section 5.5.1.3), see files labelled Tb6560videoreconstruction.mov presented in the accompanying CD.

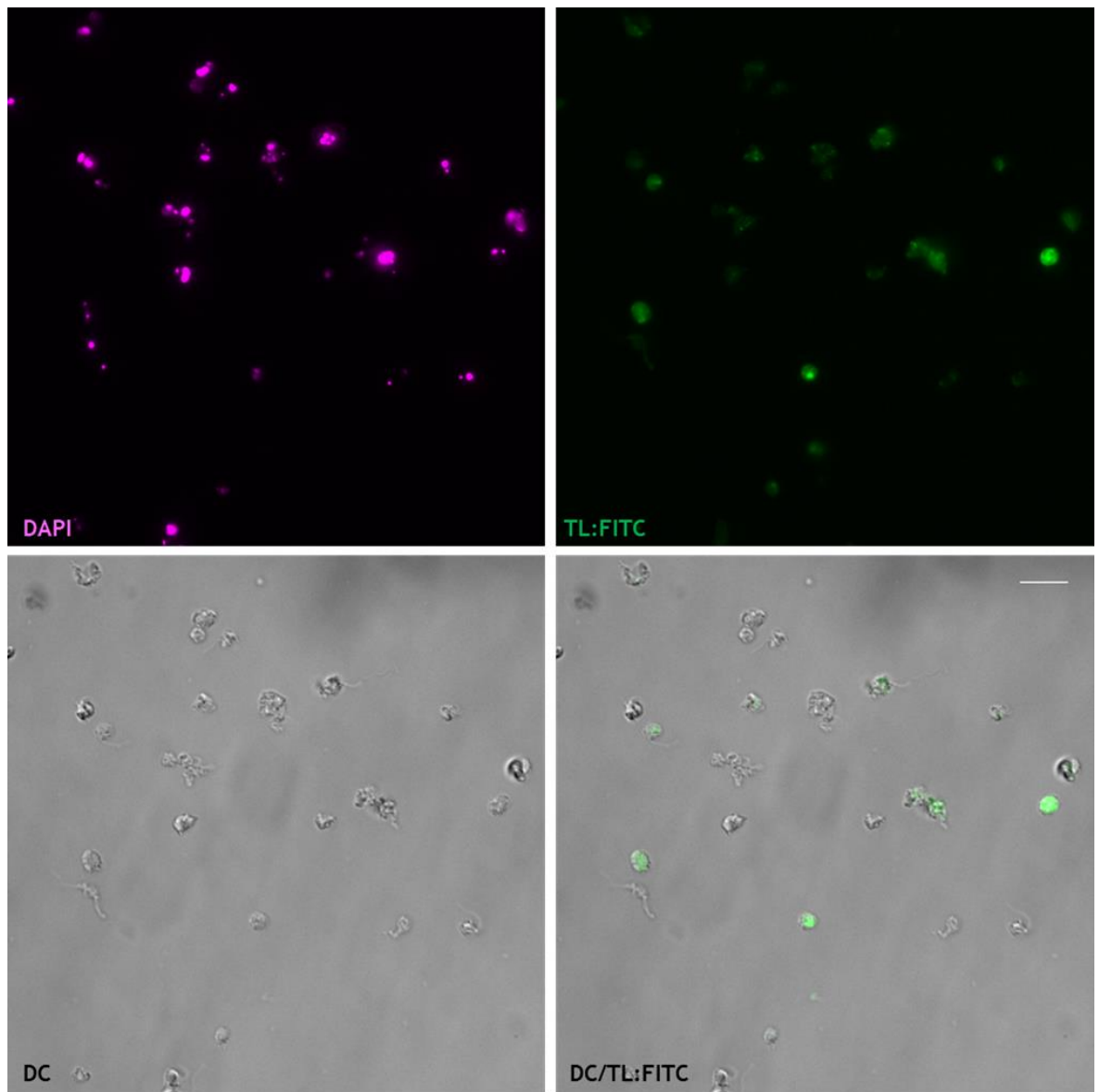
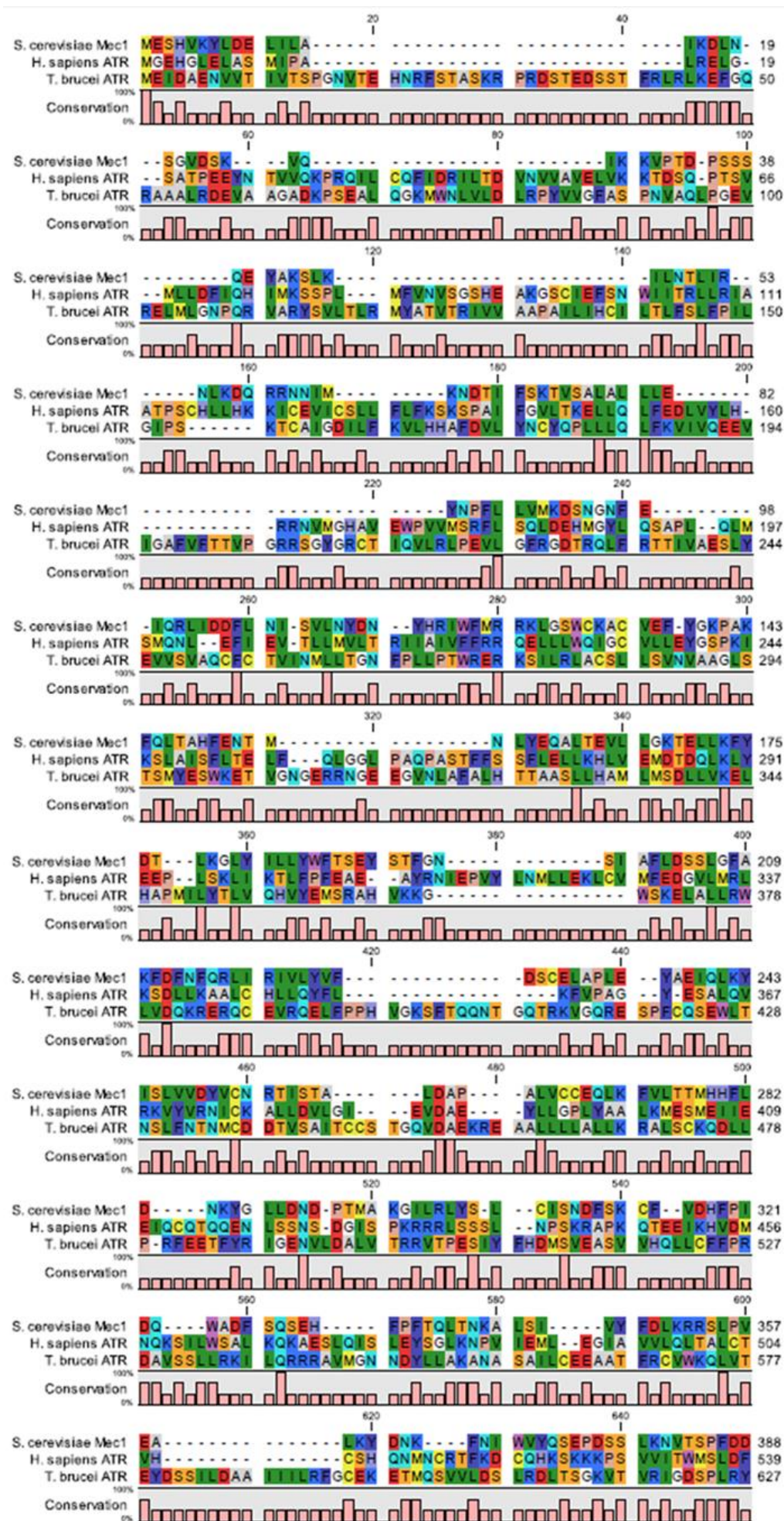


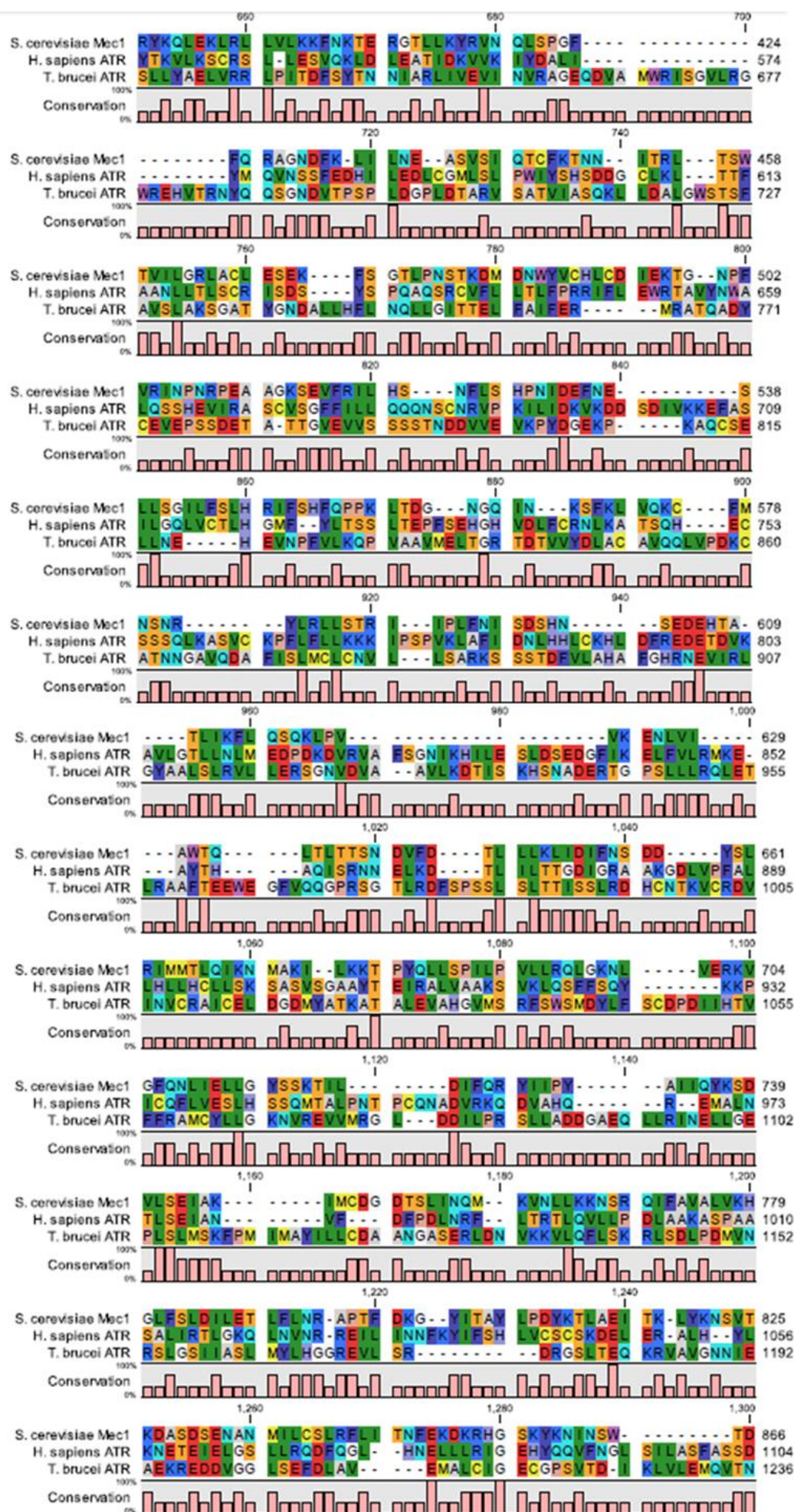
Figure 8-28: Cells lacking Tb6560 are defective in endocytosis
Representative field of view images of FITC-conjugated tomato lectin (TL) uptake in Tb6560-/- knockout cells. This assay was performed as described in section 2.11.6. DC = differential interference contrast microscopy. Images captured on an Axioskop2 and processed in ImageJ as per section 2.11.8. Scale bar = 10 μ m.

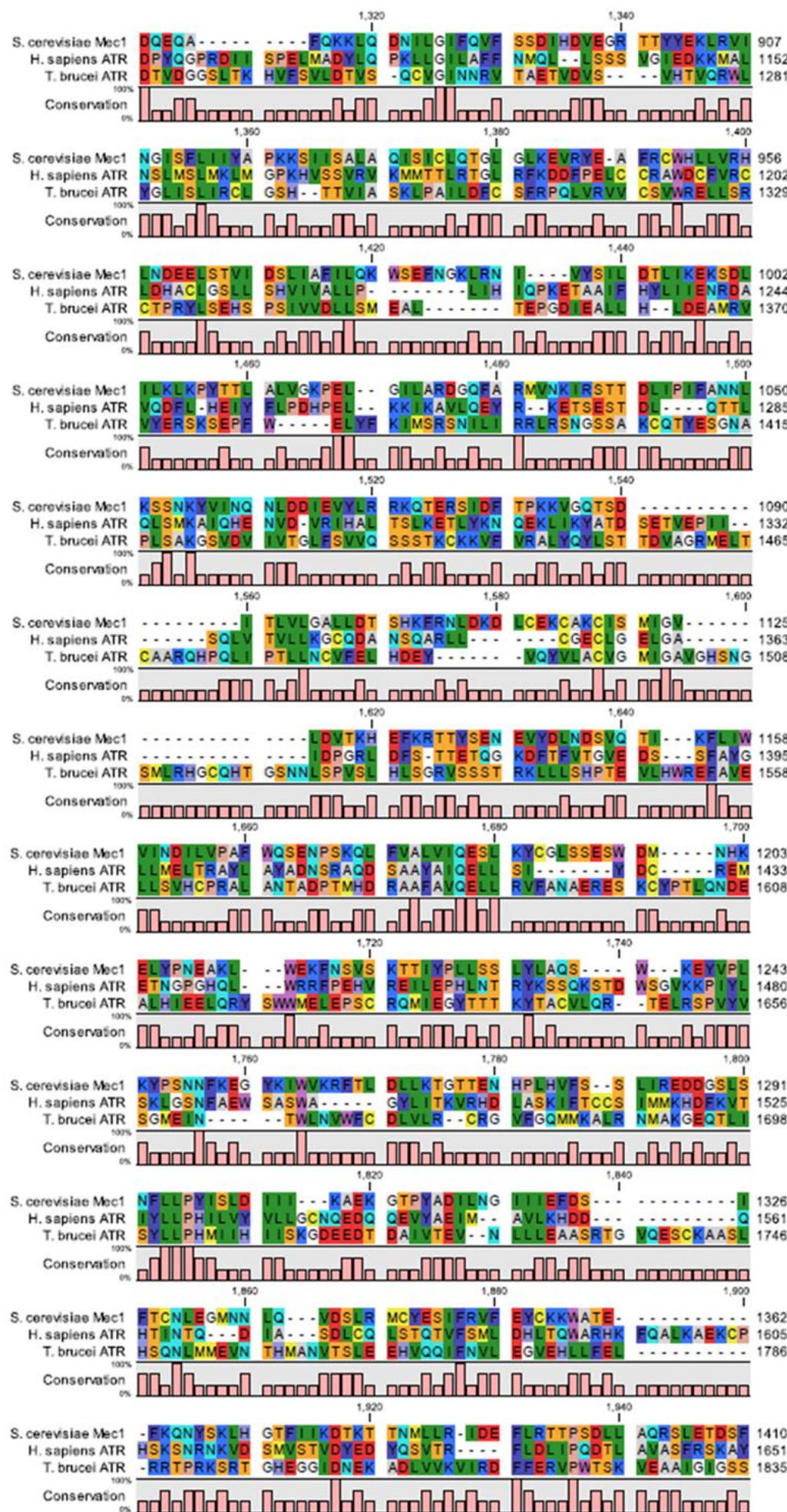
For all the raw mass spectroscopy data, see Excel file labelled MSdataTb6560andTbAUK22016.xls presented in the accompanying CD.

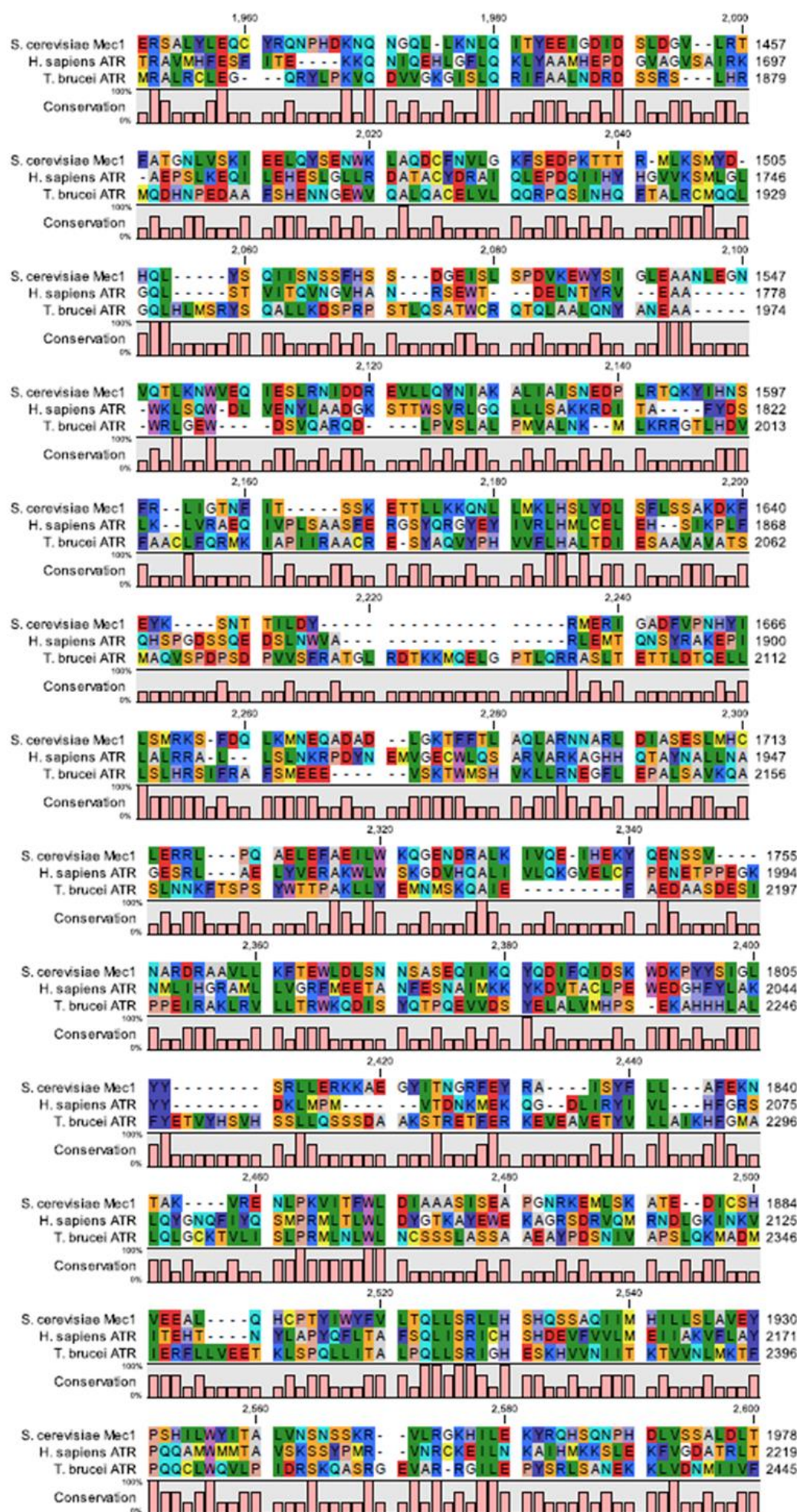
8.5 Chapter 6 appendices

The following section contains the additional material referenced in Chapter 6 (Analysis of the DNA repair associated protein kinases TbATR and TbATM in bloodstream form trypanosomes).









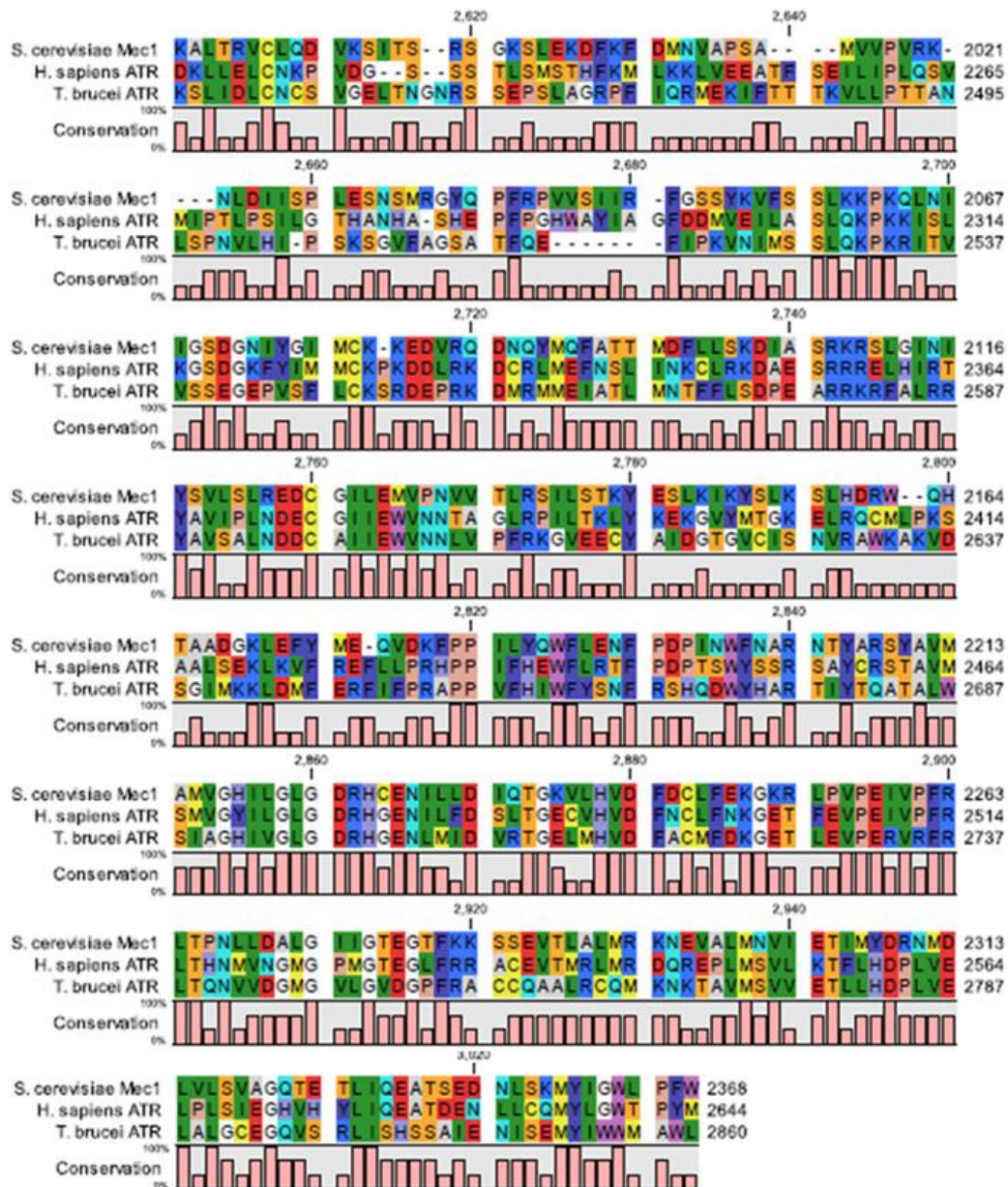
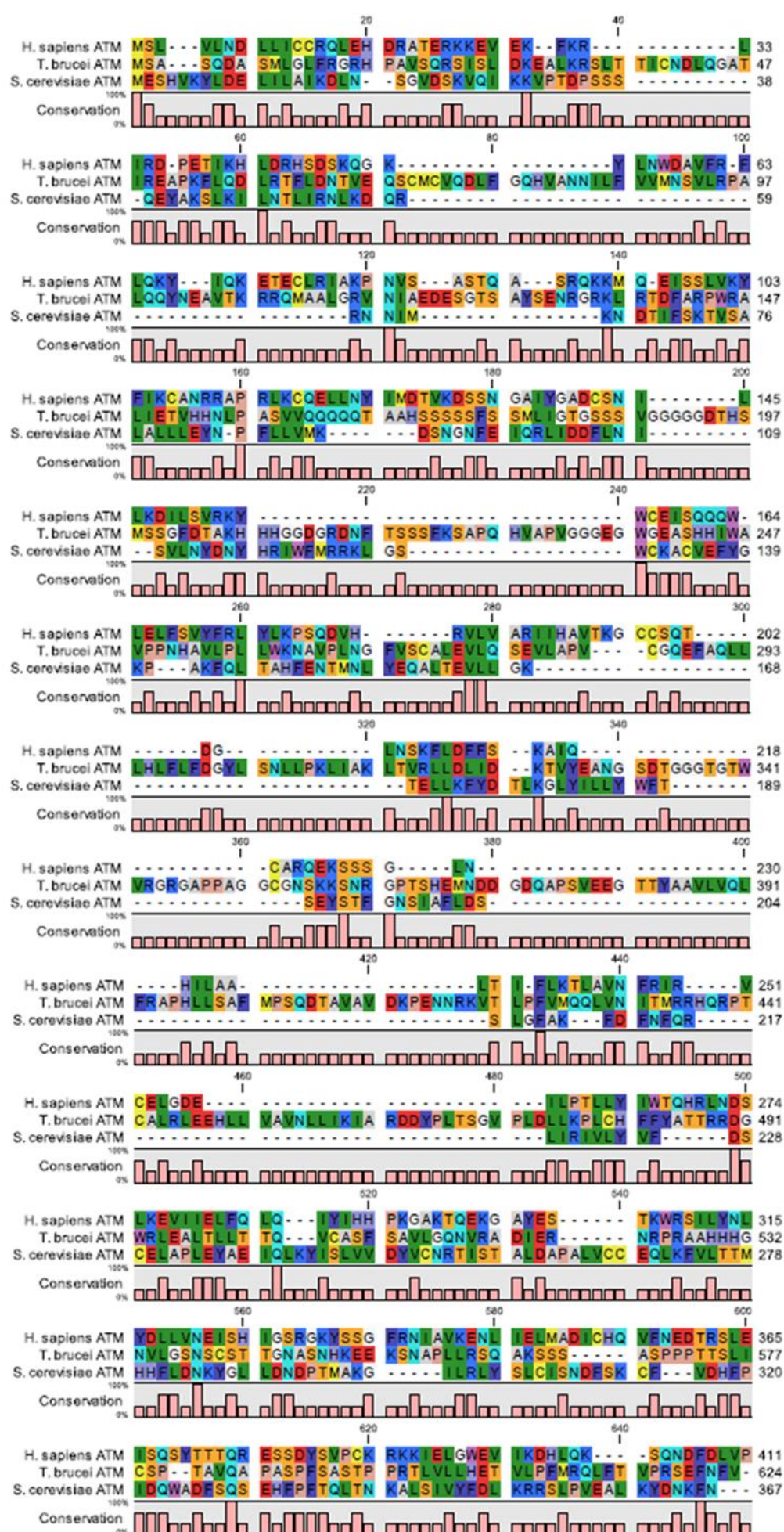
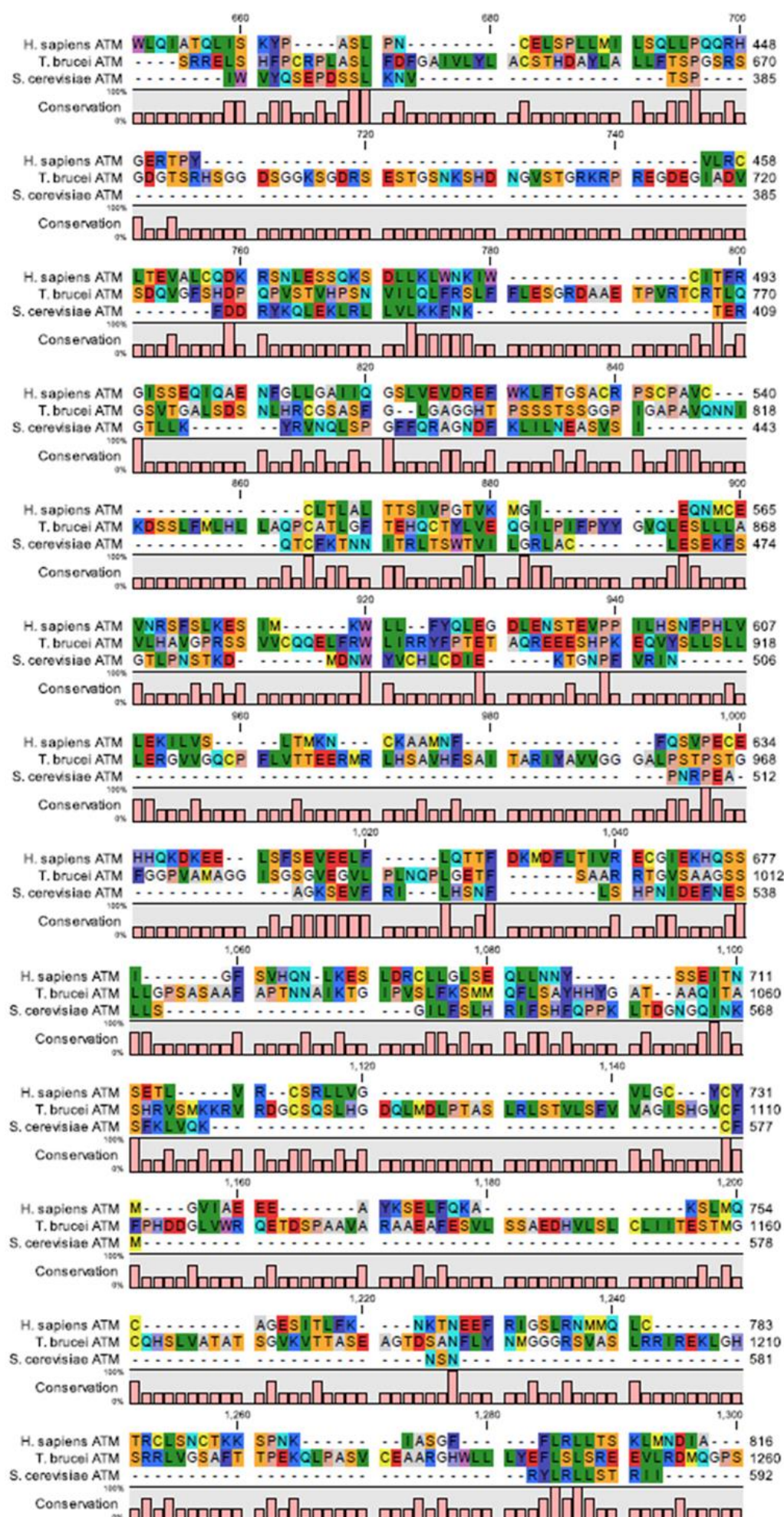
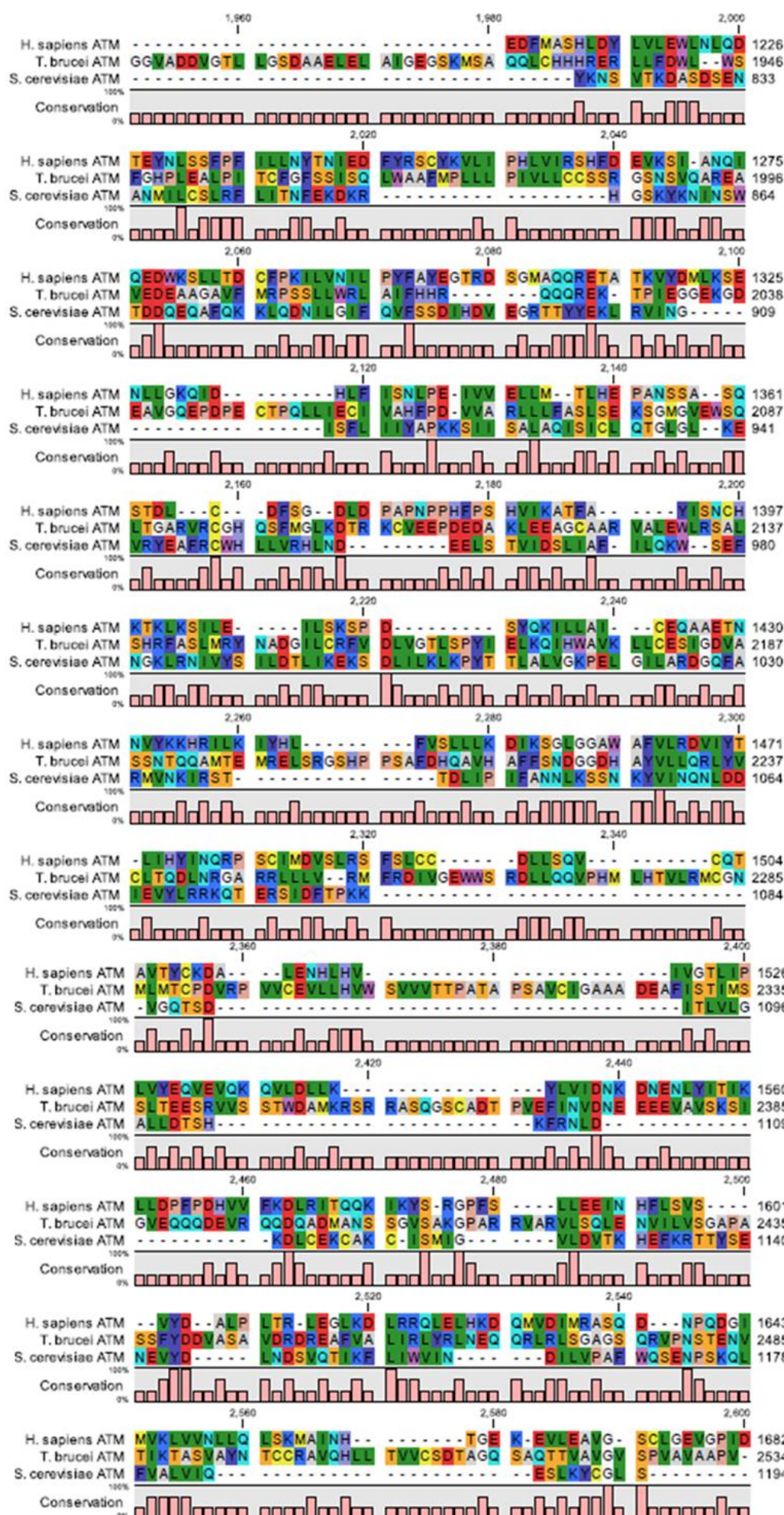
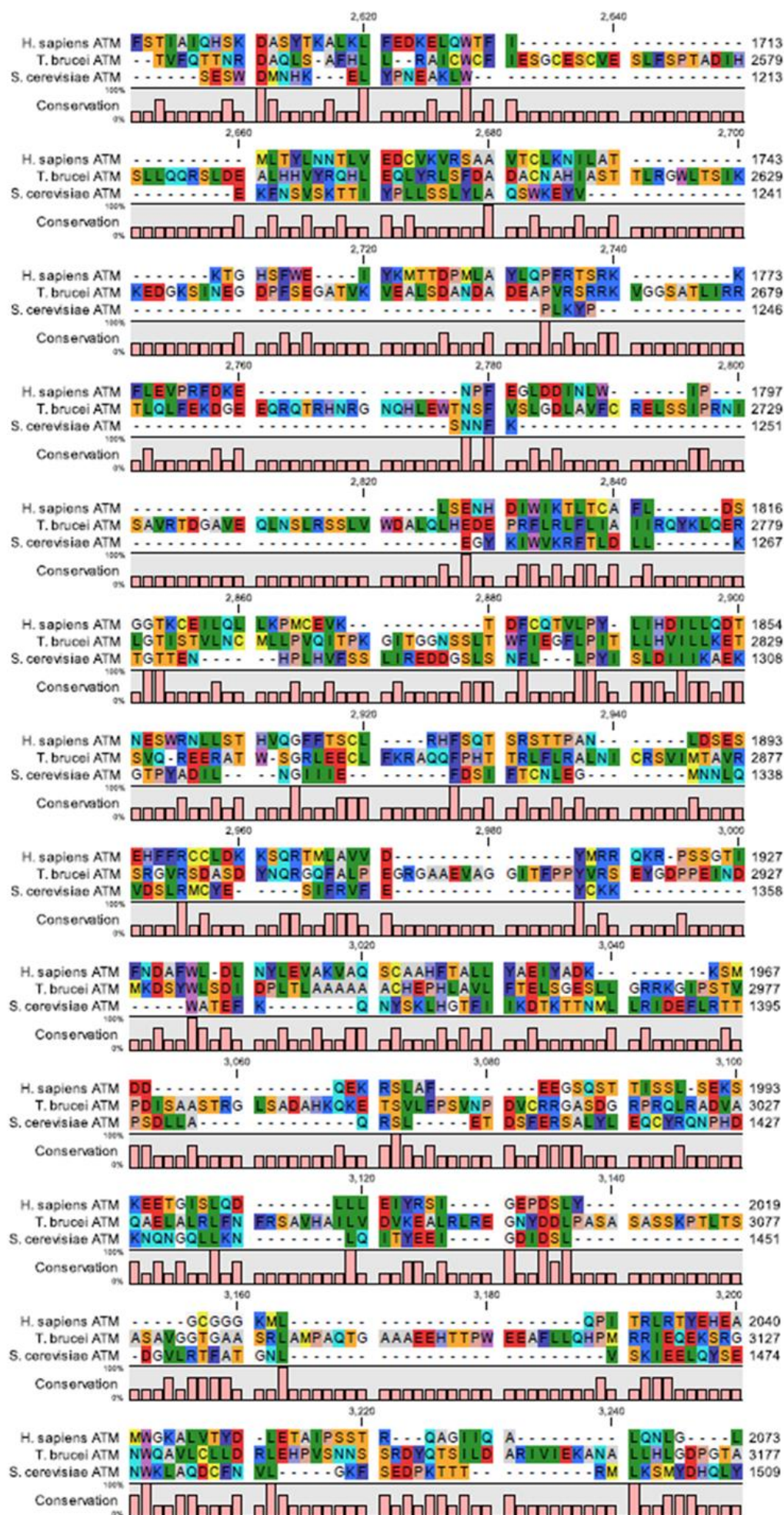


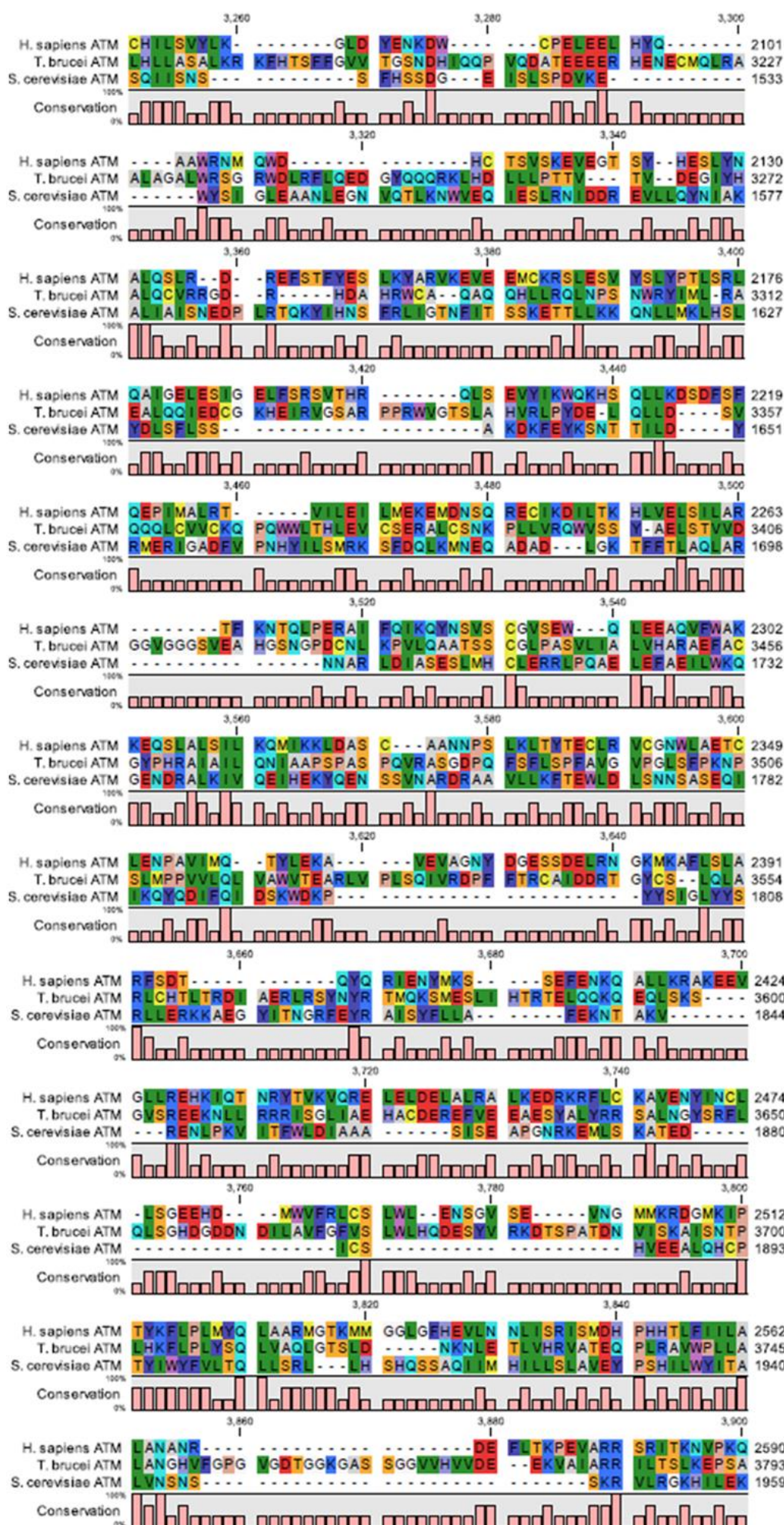
Figure 8-29: Protein sequence alignments between TbATR, Mec1 and human ATR
The protein sequences of TbATR (*T. brucei* on the diagram), Mec1 (from *S. cerevisiae*) and ATR (from *H. sapiens*) were aligned in CLC Genomics Workbench 7. The TbATR sequence was retrieved from TriTrypDB, v28. The other sequences were retrieved from the NCBI database. The consensus sequence is shown below the corresponding alignment (graph). Coloured using Rasmol colour palette in CLC Genomics Workbench 7. Accession numbers: *T. brucei* (Tb927.11.14680; TREU 927), *H. sapiens* (NP_001175.2) and *S. cerevisiae* (KZV13216.1).











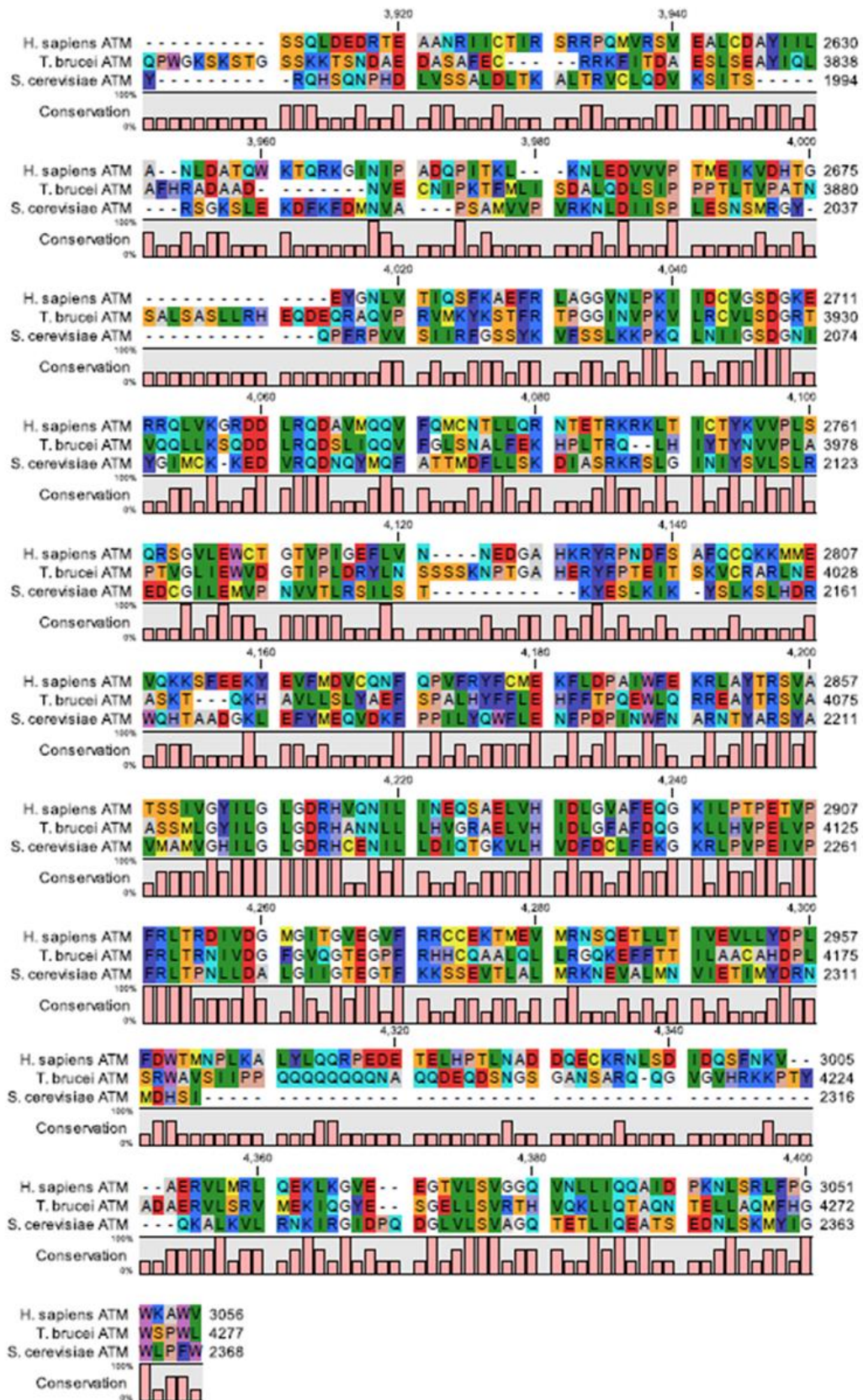


Figure 8-30: Protein sequence alignments between TbATM, the budding yeast ATM and human ATM

The protein sequences of TbATM (*T. brucei* on the diagram), ATM (also known as Tel1; from *S. cerevisiae*) and ATM (from *H. sapiens*) were aligned in CLC Genomics Workbench 7. The TbATM sequence was retrieved from TriTrypDB, v28. The other sequences were retrieved from the NCBI database. The consensus sequence is shown below the corresponding alignment (graph). Coloured using Rasmol colour palette in CLC Genomics Workbench 7.

Accession numbers: *T. brucei* (Tb927.2.2260; TREU 927), *H. sapiens* (AAB65827.1) and *S. cerevisiae* (Tel1; CAA84909.1).

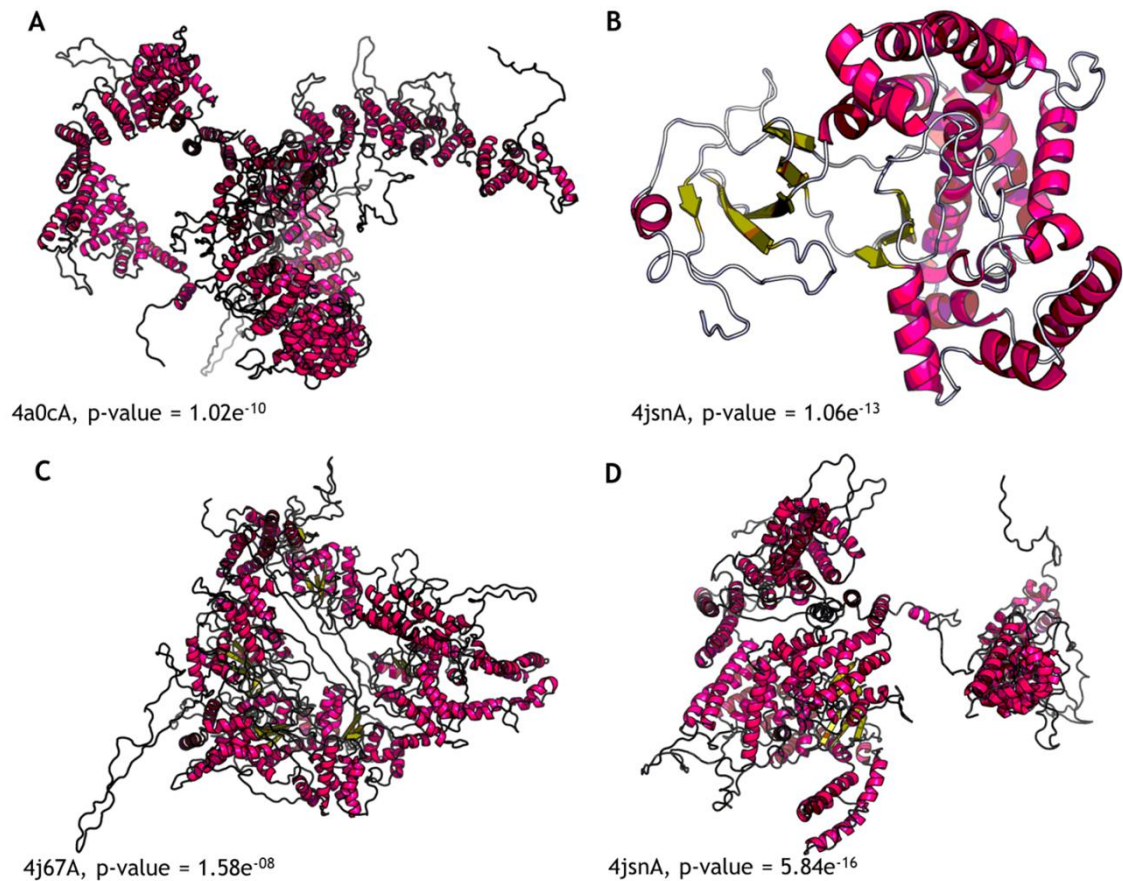


Figure 8-31: TbATR and TbATM shows structural similarity to
(A+B) Predicted 3D structural model of the TbATR protein using the RaptorX web portal
(<http://raptorx.uchicago.edu/>), as performed on in August 2016, modelling the structure from
the 1st amino acid to the amino acid in position 2477 (A) and the structure from the amino
acid in position 2478 until the final amino acid. 100 % of the residues were modelled in each
case with 3% disorder predicted for (A) and 4% disorder predicted for (B). Structural
prediction was modelled on the crystal structures of the following: 4jsn4, 5fvma, 4a0cA,
2qnaA, 1n52A and 4c9bB for (A). The best template was 4a0cA (CANDI-CHL4B-RXB1), which
was modelled with high confidence (1.02×10^{-10}). For (B) the following templates were used:
4jsnA and 5fvma. The best template was 4jsnA (mTORdelta complexed with mLST8), which
was modelled with high confidence (1.06×10^{-13}). (C+D) Predicted 3D structural model of the
TbATM protein using the RaptorX web portal
(<http://raptorx.uchicago.edu/>), as performed on
in August 2016, modelling the structure from the 1st amino acid to the amino acid in position
2499 (A) and the structure from the amino acid in position 2500 until the final amino acid.
100 % of the residues were modelled in each case with 9% disorder predicted for (C) and 5%
disorder predicted for (D). Structural prediction was modelled on the crystal structures of
the following: 4j67A for (C). The best template was 4j67A (dynein ponestroke state), which
was modelled with high confidence (1.58×10^{-8}). Structural prediction was modelled on the
crystal structures of the following: 4jsnA, 5fvma, 4CB9, 4RV1, IWA5, 9olsA (D). The best
template was 4jsnA (mTORdelta complexed with mLST8), which was modelled with high
confidence (5.84×10^{-16}).

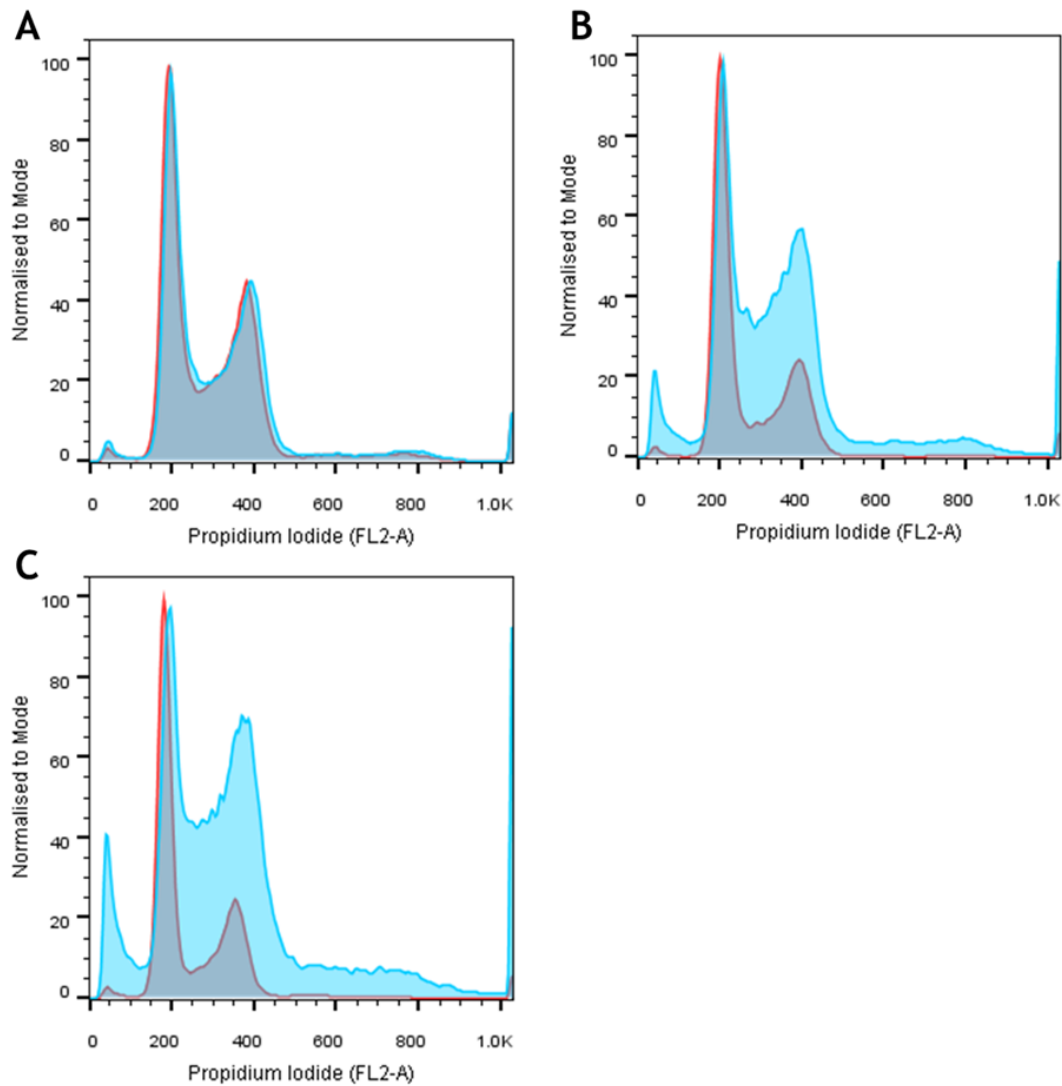


Figure 8-32: *In vitro* cell cycle analysis of TbATR

The cell cycle was examined by flow cytometry as per section 2.8.4 at 24 hrs (A), 36 hrs (B) and 48 hrs (C) post tetracycline induction. The distribution of each population of cells is according to their DNA content. 50000 events were captured with the number of cells being normalised to the mode. The DNA was stained with propidium iodide (FL-2A channel). Tet + (blue line) and Tet – (red plot) are shown as overlapped histograms. These data are from one experiment. The histograms were generated using FlowJo V10 software (<http://www.flowjo.com/>).

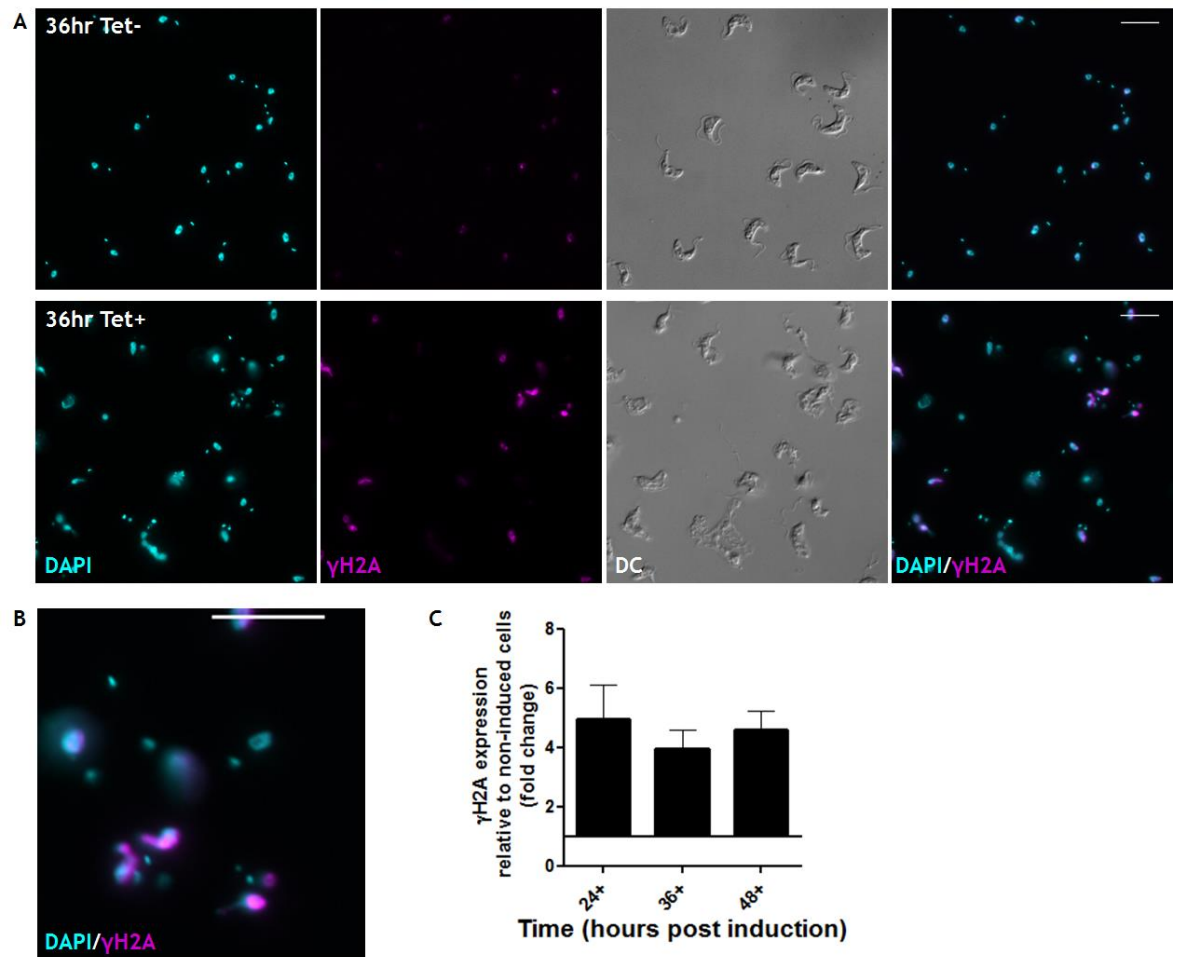


Figure 8-33: Loss of TbATR is associated with increased γ H2A expression in BSF cells (A and B) The cells were fixed and stained with α γ H2A and DAPI as per section 2.11.2. Indirect IF analysis was performed as per section 2.11.2 with γ H2A being detected with α γ H2A (magenta) antiserum (Table 2-7). The n- and kDNA were stained with DAPI (green). Cells were images on an Axioskop2 and processed as per section 2.11.8. Representative images of γ H2A localisation in induced (Tet+) and uninduced (Tet-) cells at 36 hrs post induction. An enlarged image of the induced cells is shown in B. Scale bar = 10 μ m. Images are from the TbATR CL1 cell line. (C) Quantification of western blot signal using ImageJ (as per section 2.12.5) and expressed as the fold change relative to non-induced cells at each time point. Error bars represent \pm SEM, n=2.

Sample Name	Qubit (ng/ μ l)	Nanodrop (ng/ μ l)	Nanodrop ratio 280/260	Nanodrop ratio 260/230
19047 24+	355	207.3	2.15	2.43
19047 24-	317	234.1	2.15	2.21
19047 36+	206	159.7	2.14	2.08
19047 36-	341	299.7	2.14	2.46
17970 3 24+	385	281	2.15	1.64
17970 3 24-	408	310.9	2.10	2.26
17970 2 24+	312	317.2	2.13	2.31
17970 2 24-	312	322.4	2.12	2.07
17970 2 36+	295	272.4	2.14	2
17970 2 36-	371	351	2.12	2.46
17970 1 36+	239	238	2.16	1.86
17970 1 36-	417	358.2	2.1	2.4

Table 8-5: Concentrations of RNA from each sample used for the RNAseq experiment. Sample concentration was measured as described in sectionx. 280/260 = ratio of absorbance at 280 nm and 260 nm. ~2.0 is accepted as pure RNA. 260/230 = ratio of absorbance at 260 nm and 230 nm. Generally 2.0 is accepted as contaminant free. Lower values could indicate contamination by organic compounds such as phenol.

Sample Name	Total Reads	Mapped	% mapped	Properly paired	% properly paired
24hr neg1	113025693	1.13E+08	100	61079632	93.09
24hr neg2	125263653	1.25E+08	100	67937778	94.8
24hr neg3	124207621	1.24E+08	100	68665958	94.58
24hr pos1	104184031	1.04E+08	100	54563856	91.66
24hr pos2	133423879	1.33E+08	100	72789686	95.1
24hr pos3	114392459	1.14E+08	100	63739812	94.63
36hr neg1	132937980	1.33E+08	100	71448392	94.77
36hr neg2	120523870	1.21E+08	100	64521270	94.39
36hr neg3	70620690	70620690	100	14764232	32.58
36hr pos1	112429470	1.12E+08	100	60716270	93.59
36hr pos2	137519355	1.38E+08	100	74629386	94.27
36hr pos3	116072326	1.16E+08	100	62169646	92.01

Table 8-6: FlagStat analysis of the individual RNAseq replicates
FlagStat files were generated using the FlagStat tool in the samtools set. The appropriate BAM file for each replicate was analysed in this manner. FlagStat analysis was performed by N.Dickens. Raw 'Flagstat' files are available in the accompanying CD in the folder labelled RNAseqDatasetATRBSF2016→Flagstat.

For all the files relating to the RNAseq experiment performed in chapter 6 (section 6.3.9), see files labelled RNAseqDatasetATRBSF2016 presented in the accompanying CD.

For the heatmaps referred to in chapter 6 (section 6.3.9), see files presented in the folder RNAseqDatasetATRBSF2016→ Heatmaps→ 24hr.pdf and 36hr.pdf presented in the accompanying CD.